MODELING Si/Ge INTERDIFFUSION IN $Si/Si_{1-x}Ge_x/Si$ SINGLE QUANTUM WELL STRUCTURES

MODELING Si/Ge INTERDIFFUSION IN $Si/Si_{1-x}Ge_x/Si$ SINGLE QUANTUM WELL STRUCTURES

By

Mohammad Hasanuzzaman, B.Sc., M.Sc.

A Thesis
Submitted to the School of Graduate Studies
in Partial Fulfillment of the Requirements for the Degree of
Masters of Applied Science

McMaster University
Hamilton, Ontario, Canada

To My Beloved Wife

MASTERS OF APPLIED SCIENCE (2005) McMASTER UNIVERSITY
(Electrical Engineering) Hamilton, Ontario, Canada

TITLE: Modeling Si/Ge Interdiffusion in $Si/Si_{1-x}Ge_x/Si$ Single Quantum Well Structures

AUTHOR: Mohammad Hasanuzzaman, B.Sc., M.Sc. (Bangladesh University of Engineering and Technology, Dhaka, Bangladesh)

SUPERVISOR: Dr. Yaser M. Haddara

NUMBER OF PAGES: xi, 90

ABSTRACT

Recently Silicon Germanium alloy ($Si_{1-x}Ge_x$) is showing lots of potentials in device fabrication. Most of the structures containing $Si_{1-x}Ge_x$ that are fabricated at present involve $Si/Si_{1-x}Ge_x$ heterostructure. The fabrication process involves several high temperature anneal steps in either inert, oxidizing or nitriding ambient which results the interdiffusion of Si and Ge through the hetero-interfaces. The interdiffusion causes broadening of $Si/Si_{1-x}Ge_x$ interface and changes the physical position of the hetero-interface which can cause degradation of device performance. Several studies have so far been done to quantify the amount of Ge interdiffusion in heterostructures. However no study has yet been performed to model this phenomenon. Modeling the interdiffusion mechanism is important for two reasons: (1) it will facilitate to calibrate the device characteristics taking the effect of interdiffusion mechanism into calculations prior to device fabrication; and (2) to get a better insight of the actual mechanism involved in the interdiffusion process. In this study, attempt has been taken to model interdiffusion of Si and Ge in structures having $Si/Si_{1-x}Ge_x$ hetero-interfaces. Mathematical models are proposed to model the behavior and the models are applied to previously published results where samples were annealing in inert, oxidizing and nitriding ambient at different anneal temperatures for different anneal times. First only the contributions of vacancies in the interdiffusion mechanism are considered. This can successfully model the interdiffusion mechanism for samples annealed in inert and oxidizing ambients at low temperatures (below 1050°C). Next the contributions of interstitials along with vacancy in the interdiffusion mechanism are considered. These are able to successfully model the interdiffusion phenomenon for the samples annealed in oxidizing and nitriding ambients

at high temperatures (above 1050°C). The success of the modeling is justified by getting good match between the simulated and the experimental interdiffusion profiles along with good match between the fitting parameters used in the simulations compared with previous reported values. Besides modeling the interdiffusion mechanism, for the first time, a mathematical model is proposed for vacancy injection while nitridation of silicon is done.

ACKNOWLEDGEMENTS

I wish to thank and offer my heartiest gratitude to my supervisor Dr. Yaser M. Haddara for giving me the opportunity to work with him and his continuous guidance, suggestions and wholehearted supervision throughout the progress of this work. Despite of his busy schedules, he always tried to provide me time to discuss the progress of the work when requested.

I would like to thank all of my group mates in our research group for the continuous support and fruitful discussions during doing this work.

I want to thank my parents Akhtaruzzaman and Hasina for their support and encouragement to complete the work. I would like to thank my wife Farhana; her presence with me in Canada and her continuous encouragements really helped me a lot to give concentrations to do this work. I would also like to thank my sister Afreen for her support and encouragements.

Finally, I am grateful to the Almighty for giving me the strength and courage to complete the work.

TABLE OF CONTENTS

LIST OF FIGURES

LIST OF TABLES

Chapter 1

INTRODUCTION

1.1 Background

Silicon (Si) has long dominated the semiconductor industry. Along with low fabrication cost technology, the properties of silicon oxide and silicon nitride, two insulators that may be thermally grown on Si, also favor the use of silicon in integrated circuit technology. Silicon and its insulators allow highly conformal growth, high uniformity of selective etching, and high deposition yield. Though the first solid state transistor was fabricated in germanium (Ge), and other semiconductor materials may have higher mobilities, these considerations have allowed Si to dominate the semiconductor industry to date.

In April of 1965, an article by Intel co-founder Gordon Moore was published in *Electronics* magazine where he observed an exponential growth in the number of transistors used per integrated circuit and predicted this trend to continue [1]. The way this trend is most commonly described is "the number of transistors that can be fit onto a square inch of silicon doubles every 12 months", which is known as Moore's law a trend that has continued to hold to the present day.

The dominant Si technology platform is CMOS. Complementary metal oxide semiconductor, which uses both p- and n- channel field effect transistors to create logic gates that have low leakage currents and dissipate power only during switching. The low current is mainly achieved by using high quality insulators like silicon oxide and silicon nitride. CMOS scaling has thus far been accomplished by shrinking geometry and increasing dopant densities in tandem. Given the performance requirements of future technology generations, purely geometrical scaling is no longer possible, and industry has recognized the necessity of incorporating new materials to continue CMOS scaling [2].

Additionally, there are application areas where materials other than Si have maintained niche dominance. For example, in radio frequency (RF) power amplifiers and lasers, gallium arsenide (GaAs) and indium phosphide (InP) are widely used for their speed advantages, as well as the ease of manufacturing lattice-matched heterostructure devices with even higher performance. However, these alternative technologies remain limited in their application by the high cost of manufacturing.

The interest in silicon-germanium (SiGe) technology has grown due to its potential in meeting both of these challenges: its incorporation in CMOS technology can overcome some of the barriers to scaling (e.g. by reducing the resistivity of the source and drain regions) and it offers a low-cost high-speed solution. The primary advantage of SiGe is that it can easily be integrated with the mature and low cost Si fabrication processes. Also due to the high electron mobility in SiGe compared to Si, SiGe shows lots of potentials in RF applications and becoming a competitor of high cost III-V materials.

1.1.1 SiGe Material Properties: Strain, Critical Thickness and Dislocations

Si and Ge both crystallize in the diamond crystal structure. Si and Ge are completely miscible forming solid solution of $Si_{1-x}Ge_x$ with x ranging from 0 to 1. There is a lattice mismatch between Si and Ge, the Ge lattice constant being 4.2% bigger than Si. Vegard's rule [3] is a reasonable approximation to determine the lattice constant of $Si_{1-x}Ge_x$ which is given by,

$$a(x)_{Si_{1-x}Ge_x} = xa_{Ge} + (1-x)a_{Si} \tag{1.1}$$

According to this law the lattice constant of $Si_{1-x}Ge_x$ is calculated by a linear fit between the lattice constants of Si and Ge. The lattice constant of $Si_{1-x}Ge_x$ is always greater than that of Si. Vegard's rule agrees very well with the experimentally determined lattice constant and variation of Vegard's rule with the experimental value is only about 1.8×10^{-4} %. The experimentally determined lattice constant is given by [4],

$$a_{Si_{1-x}Ge_x} = 0.0002733x^2 + 0.01992x + 0.5431 \quad \text{(nm)} \tag{1.2}$$

When an epitaxial layer of $Si_{1-x}Ge_x$ is grown on Si substrate, there is a lattice mismatch between the epitaxial layer and the substrate. Due to the lattice mismatch, lattice distortion is created in the grown $Si_{1-x}Ge_x$ epilayer. The epilayer is compressed in lateral direction and extended in vertical direction as shown in Figure 1.1.

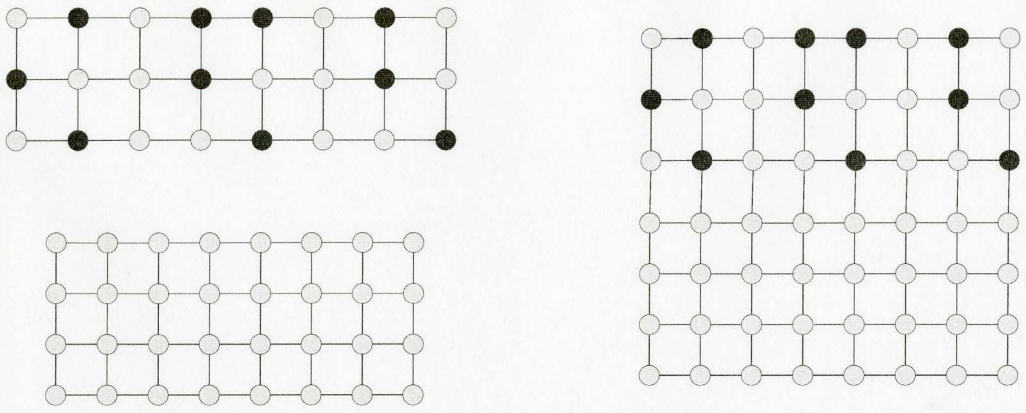

Figure 1.1: Lateral distortion due to lattice mismatch. The top $Si_{1-x}Ge_x$ layer is under compressive strain when grown on Si substrate [5].

The epilayer grown in the way shown in Figure 1.1 is in compressive strain. When a thin $Si_{1-x}Ge_x$ is grown on top of $Si_{1-y}Ge_y$ film, for $x > y$, the top layer is compressively strained like in Figure 1.1. If a Si epilayer is grown on $Si_{1-x}Ge_x$ or a $Si_{1-x}Ge_x$ is grown on top of $Si_{1-y}Ge_y$ film with $x < y$, the top layer will be in tensile strain as shown in Figure 1.2.

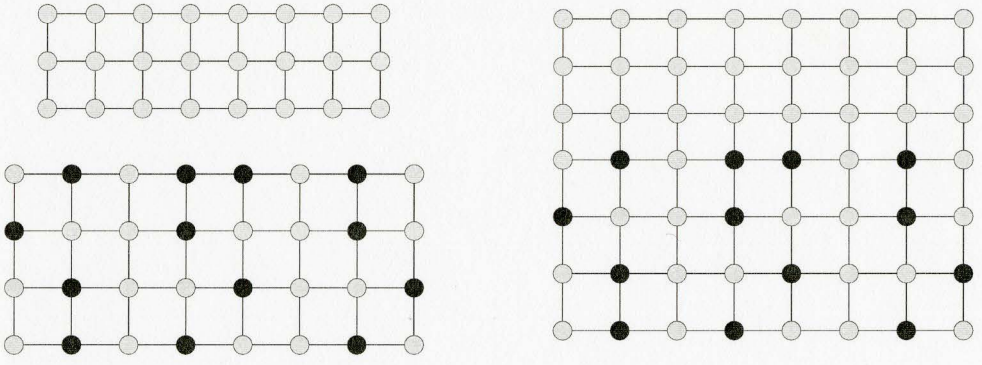

Figure 1.2: Lateral distortion due to lattice mismatch. The top Si layer is under tensile strain when grown on $Si_{1-x}Ge_x$ substrate [5].

Initially the grown films are pseudomorphic in nature. By pseudomorphic it is meant that the lattice mismatch present between the epilayer and substrate is totally accommodated by the strain without forming any misfit dislocation. This remains the case for film thickness up to a certain "critical thickness" beyond which the film tends to relax forming misfit dislocations. There is a metastable region where the grown film remains strained as it is grown, but relaxes upon annealing the sample. Figure 1.3 shows the critical thickness of $Si_{1-x}Ge_x$ grown on bulk (100) Si as a function of Ge fraction.

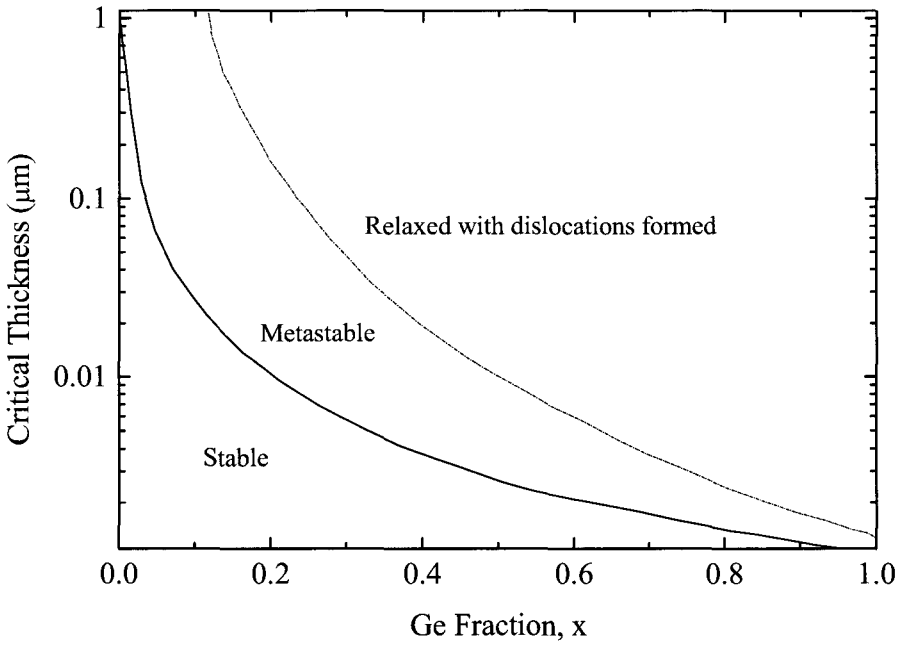

Figure 1.3: Critical thickness as a function of Ge fraction for $Si_{1-x}Ge_x$ layers grown on bulk (100) Si [5].

For an epilayer grown with a thickness greater than the critical thickness, misfit dislocations cause relaxation of strain. A relaxed epilayer forming misfit dislocations is shown in Figure 1.4.

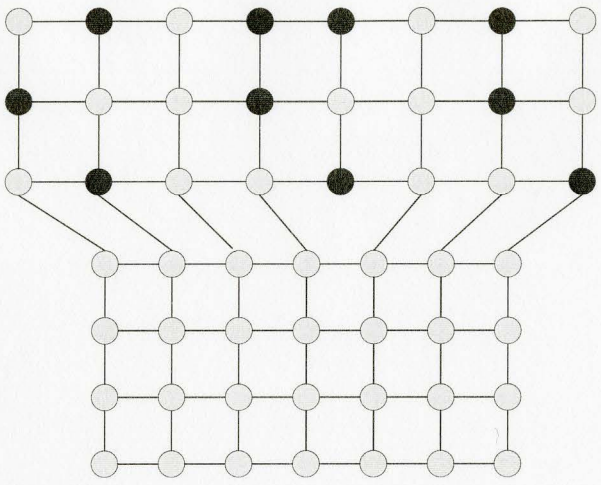

Figure 1.4: Relaxed top layer creates misfit dislocations in the structure.

The lattice mismatch, f can be described as,

$$f = \frac{a_{relaxed} - a_{substrate}}{a_{substrate}} \tag{1.3}$$

where, $a_{relaxed}$ is the lattice constant of relaxed epilayer and $a_{substrate}$ is the lattice constant of substrate.

1.2 Motivation Behind the Study

The possibility, outlined in the previous section, of producing pseudomorphic $Si/Si_{1-x}Ge_x$ heterostructures has allowed the fabrication of devices that make use of the bandgap narrowing and band offsets resulting from compositional gradients and the strain in the structure. One of the most important devices is the SiGe heterojunction bipolar transistor (HBT) where SiGe forms the base and Si forms the emitter and the collector regions. Using $Si_{1-x}Ge_x$ in the base of a $Si/Si_{1-x}Ge_x/Si$ npn-transistor lowers the potential barrier for injected electrons from emitter to base while retaining a high barrier to the

injection of holes, thus increasing the emitter efficiency, and hence the speed of the transistor. The lower energy bandgap of $Si_{1-x}Ge_x$ causes an exponential increase in the current gain of the transistor for a constant emitter base voltage drop. Additional speed advantages arise from the higher electron mobility in the SiGe layer, and from additional field enhancement if the Ge profile in the base is graded. Besides these, one of the major concerns in device fabrication is the cost associated with the fabrication process. Fortunately $Si/Si_{1-x}Ge_x$ heterostructure devices can be fabricated using the well developed low cost Si process lines which results low cost for fabricating these devices. The typical cost associated with fabrication of SiGe hetero-devices is \$ 0.12/mm^2, which is slightly higher than the fabrication cost \$ 0.09/mm^2 associated with Si device, both of these costs are much less than the fabrication costs of InP and GaAs which are typically as high as \$ 1.2/mm^2 and \$ 0.5/mm^2 respectively [6].

However, integrating SiGe HBTs with a conventional CMOS fabrication process means that device fabrication will involve several high temperature annealing steps. The interdiffusion of Si and Ge during such high temperature steps can lead to a broadening of the $Si/ Si_{1-x}Ge_x$ interface and can cause a shift in the position of the interfaces. This can have a negative impact on the device characteristics, for example by causing a misalignment of the Ge profile and the dopant profile so that the emitter-base junction no longer becomes a heterojunction. However Si-Ge interdiffusion can be beneficial to device operation, for example, in SiGe quantum dots where controlled interdiffusion may be utilized in tuning optical properties [7]. So far, much experimental work has been performed to quantify Si-Ge interdiffusion in $Si/ Si_{1-x}Ge_x$ heterostructures. However,

none of these studies focused on modeling Si-Ge interdiffusion phenomena. Modeling Si-Ge interdiffusion is the primary focus of this thesis.

1.3 FLOOPS-ISE

FLorida Object Oriented Process Simulator (FLOOPS) [8] a process simulator commercially developed by Integrated System Engineering (ISE), is used as the simulator in this study. Commercially the name of this simulator is given FLOOPS-ISE. This simulator is capable of simulating all standard process simulation steps such as implantation, deposition, oxidation, etching, diffusion and silicidation. A grid is defined for a region of interest, and mathematical equations are solved within this grid. The accuracy of the simulation greatly depends on the fineness of the defined grid. The material and the model parameters of the simulator are contained in a parameter database. The simulator allows access to the parameter database and gives the option to use values other than the default values defined for the parameters in the parameter database. For our purposes, our main concern is its ability to simulate diffusion phenomena. There are six predefined diffusion models in FLOOPS-ISE which are-*Constant*, *Fermi*, *Pair*, *React*, *ChargedFermi* and *ChargedPair*. The default model is *Fermi* model which considers point defects remain in equilibrium. As in our model the effects of point defects in the diffusion mechanism are considered, it is necessary to solve the point defect equations, thus the diffusion model is switched to *Pair* diffusion model which allows to do this.

To do simulations in FLOOPS-ISE, it is necessary to initialize all the diffusing parameters and to set appropriate boundary condition. FLOOPS-ISE has six boundary conditions defined in it which are – *HomNeumann*, *Natural*, *Dirichlet*, *Segregation*, *ThreePhaseSegregation*, and *Epitransfer*. *HomNeumann* boundary condition which can

be applied to any boundary assumes no flux transfer across the boundary. This is by default chosen at left, right and bottom boundary of the structure. At the top surface *Natural* boundary condition is applied for vacancy and Si interstitial.

For our application we made use of the Alagator Scripting Language that allows a user to incorporate user-defined partial differential equations and boundary conditions to use with diffusion simulations. In our case this was necessary to experiment with implementations of our proposed models, which are not available by default.

1.4 Thesis Layout

In the forgoing section we have outlined our motivation for studying Si-Ge interdiffusion and gave a brief survey of the significance of SiGe heterostructures, as well as a brief introduction to the process simulator used in our study.

Chapter 2 provides a survey of point defects and diffusion in semiconductors while Chapter 3 is a review of studies of self-diffusion in Si, Ge, and SiGe, as well as Si-Ge interdiffusion in heterostructures. We have focused our study on modeling experimental data discussed by Griglione *et al.* [43]-[44] and Ijzendoorn *et al.* [37]. At the end of Chapter 3 we explain the rationale for focusing on these data, and we describe the device structure and detail the extraction of experimental data.

The details of the mathematical models applied in this study are described in Chapter 4. The chapter begins with the details of the derivation steps of the simple vacancy exchange model for diffusion. Next this model is modified by incorporating the contributions of interstitials in diffusion mechanisms along with the contribution of vacancies.

The simulation results based on the mathematical equations described in Chapter 4 are described in Chapter 5. The chapter starts with a description of the simulation approach taken in this study. Next the results corresponding to simulations done at temperatures below 1050°C in inert and oxidizing ambient are provided. This is followed by the results for simulations done at temperatures above 1050°C in inert, oxidizing and nitriding ambients.

Finally, Chapter 6 gives concluding remarks together with suggestions for future works.

Chapter 2

POINT DEFECTS AND DIFFUSION PHENOMENA

Point defects play an important role in device physics. In every material, diffusion of host and dopant atoms is observed to occur to some extent. To diffuse, these atoms depend on the point defects. Thus it is important to understand the behaviors of the point defects and their influences on the diffusion phenomena. In this chapter a brief description of different types of commonly seen point defects are described. Descriptions on different types of diffusion mechanisms are then provided. The chapter concludes with a description on the non-equilibrium formulation of point defects during different experimental conditions.

2.1 Point Defects

Generally, point defect can be defined as an entity causing interruption in the lattice periodicity. Point defects can be broadly divided into two categories: native point defects and impurity related point defects.

Native point defects exist at host material where imperfections in the host atoms are formed. Most commonly seen native point defects are – vacancy, interstitial and interstitialcy. Vacancy is an empty lattice site. When a host atom is removed from its

regular lattice site, a vacancy is created at the original position of the host atom. When a host atom resides at a different position than the substitutional lattice position, it gives rise to self-interstitial or intrinsic point defect. On the other hand, two atoms in non-substitutional sites around a regular substitutional lattice site create a self-interstitialcy. A point defect is considered isolated when it resides far from a dopant so that the presence of the dopant cannot alter the properties of the point defect. Point defects are called associated when the presence of the dopant can change their properties.

When foreign impurities are introduced impurity related point defects are created. Group-V elements: arsenic (As), antimony (Sb) and phosphorus (P) and group-III elements: aluminum (Al), gallium (Ga), boron (B) and indium (In) have very important role as impurities as these elements are used as dopants in semiconductor devices. These dopants readily take substitutional position in the Si lattice sites. Dopant atoms residing at substitutional sites are known as substitutional defects. When the dopant atoms occupy sites different from the usual substitutional sites, an extrinsic defect is created. Various other kinds of point defects may form in combination of the above described point defects. For example: two vacancies adjacent to each other forms divacancy, a vacancy close to a self-interstitial forms Frenkel pair. Figure 2.1 shows schematic representation of different types of point defects.

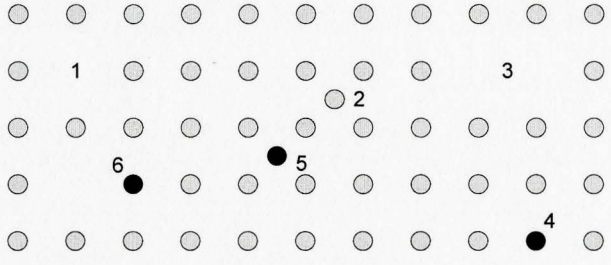

Figure 2.1: Schematic representation of point defects. (1) vacancy, (2) self-interstitial, (3) divacancy, (4) substituitional impurity, (5) interstitial impurity, and (6) vacancy-substituitional impurity complex [9].

2.2 Diffusion Mechanisms

For diffusion studies it is important to understand the atomistic mechanism by which species through the crystal lattice diffuse. There are several mechanisms by which diffusion can occur. One of the most well accepted diffusion mechanisms is vacancy exchange mechanism. In this mechanism, substitutional atom migrates to the adjacent lattice site only if its adjacent lattice site is vacant, the atom and the vacancy interchange their positions. Figure 2.2 shows a schematic representation for this mechanism. The amount of diffusion occurring through this mechanism greatly depends on the availability of a vacancy near by a host atom. However, the exchange mechanism is not as simple as only this exchange process. If only the exchange mechanism between the substitutional atom and the vacancy is the concern then there might be a situation where only exchange between a substitutional atom and a vacancy alternatively occurs and ultimately no long term diffusion is observed, which is not the situation in reality. The vacancy must diffuse away some distance away from the original substitutional atom with which it exchange the position once so that this vacancy is no longer available to that substitutional atom to exchange immediately the position again. This vacancy might come to adjacent to this substitutional atom at a different adjacent lattice position through a different path later during the vacancy exchange process.

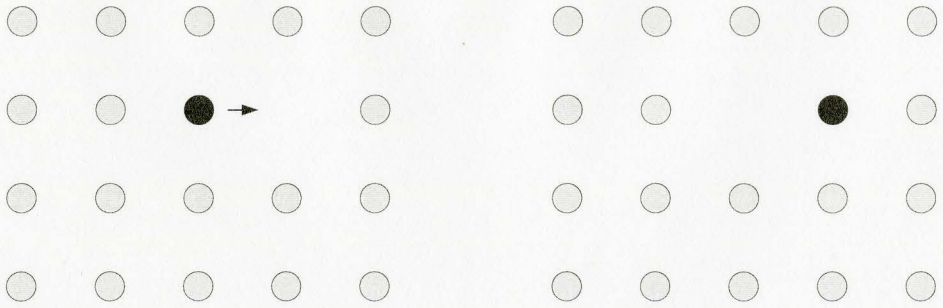

Figure 2.2: Vacancy exchange mechanism. ● is a host atom or a dopant atom taking part in the vacancy exchange mechanism [10].

Another mechanism for diffusion to occur is direct interstitial mechanism where an interstitial host atom or a dopant atom residing at interstitial site moves from one interstitial site to other interstitial site through the lattice as shown in Figure 2.3 (a). This mechanism is energetically favorable when the size of the diffusing atoms is much less than the host lattice atoms. Lattice distortion is created if the size of the atom is large and this makes the total diffusion process to be unfavorable. When the interstitial atom moving through the interstitial positions of the lattice recombines with a vacancy then the process is known as recombination mechanism. The process is shown in Figure 2.3 (b). This mechanism is both interstitial and vacancy dependent.

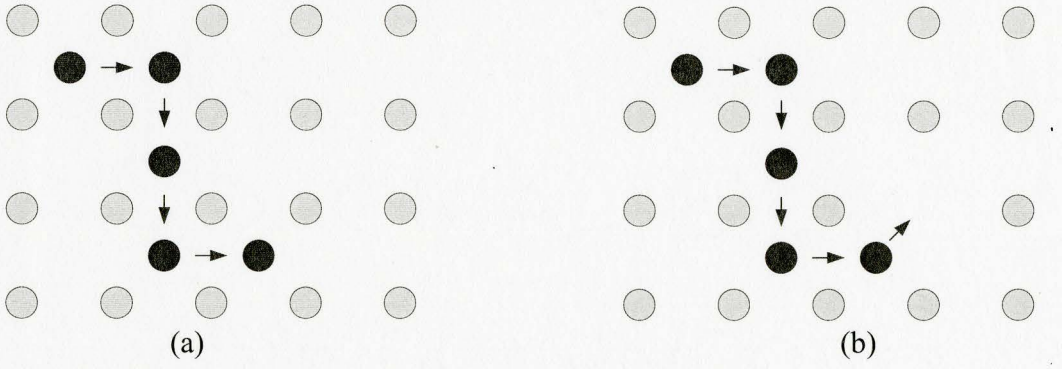

Figure 2.3: (a) Direct interstitial mechanism, (b) recombination mechanism. ● is a host atom or a dopant atom taking part in the diffusion process [10].

There is another diffusion mechanism which is seen to occur by substitutional/interstitial interchange mechanism is shown in Figure 2.4. In this mechanism an atom in the interstitial site migrates through the interstitial positions of the lattice, knocks off a substitutional atom to interstitial position and the interstitial atom takes the substitutional position. The newly created interstitial then keeps migrating through the interstitial sites until it takes a substitutional position by knocking off another host atom to interstitial position. And this process continues. This mechanism is also called "kick-out mechanism". The mechanism is only dependent on interstitial concentration.

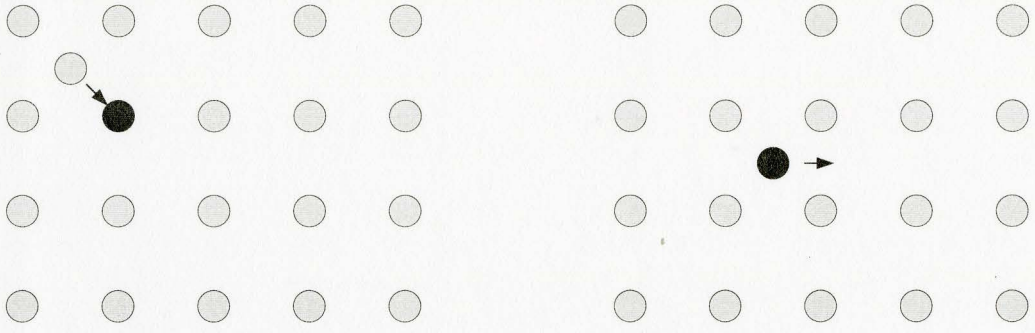

Figure 2.4: Kick-out mechanism. ● represents an atom initially at substitutional site which later becomes interstitial.

Another mechanism by which diffusion can occur is by substitutional/interstitialcy mechanism. In this mechanism a host interstitialcy atom approaches to a substitutional atom and forms interstitialcy like defect, which then migrates in the same fashion of host interstitialcy.

2.3 Injection of Non-Equilibrium Point Defect

The diffusion of host atoms and the dopants need the assistance of point defects to diffuse. Thus it is also important to study the behavior of point defects under different experimental conditions as any change in the point defect behavior simultaneously affects the diffusion behaviors of host and dopant atoms. It is commonly accepted that oxidizing Si injects interstitials whereas nitridation of Si injects vacancies. However it is not possible to track the injection of vacancy or interstitial directly. To observe these injections, diffusion of dopants are observed; for example: increase in Sb diffusion indicates injection of vacancies and increase in B diffusion indicates injection of interstitials.

Historically the enhanced diffusion of B and P due to the oxidation of Si was considered as anomalous enhanced diffusion phenomena. One of the earliest reports which mentioned this phenomenon was by Nicholas [11] back in 1966. He observed that oxidation caused rapid increase in the depth of P and B and proposed that oxidation of Si was behind this behavior of P and B. Masetti *et al.* [12] observed increased phosphorus diffusion in <111> Czochralski Si for oxidization done in the temperature range 1000-1200°C. They reported increase in phosphorus diffusion in oxidizing ambient compared to similar inert ambient case. As phosphorus and boron diffuses only in the presence of interstitials, the increase in phosphorus and boron diffusion indicates supersaturation of interstitials due to oxidation of Si. The orientation dependence of Si on oxidation process was studied by Hill [13] where the increase in diffusion enhancement of boron under oxidizing ambient was reported to occur in the order <111>, <110>, <100> during dry oxidation. The only situation where retarded diffusion was observed in oxidizing ambient

was in <111> orientated Si annealed above 1150°C. Francis and Dobson [14] observed enhanced diffusion of antimony and retarded diffusion of phosphorus and boron for <111> oriented Si wafer annealed above 1150°C. As antimony is known to diffuse only via vacancies, this above findings suggests that for the above condition, vacancy supersaturation is created in Si, thus under-saturation of interstitials are created, and there is a corresponding retardation of phosphorus and boron diffusion.

There are several theories describing the interstitial injection phenomenon in Si oxidation process. However none of these theories are supported by the experimental evidence. Hu [15] proposed a theory describing the interstitial injection phenomenon in Si. He suggested that during oxidation process a fraction of Si is displaced from the regular lattice position. These displaced Si atoms do not oxidize but approaches towards SiO_2/Si interface and becomes interstitial Si. Dunham and Plummer [16] proposed that interstitials are created during oxidation of Si which accumulate near the SiO_2 interface. These interstitials ultimately diffuse in the bulk due to the difference of the rate of interstitial diffusion into the oxide and the interstitial creation, which results supersaturation of interstitials into the bulk due to the oxidation process. Though there is yet no well accepted theory for interstitial injection due to oxidation of Si, for the purpose of this study, it is enough to accept that interstitials are indeed injected during the oxidation of Si.

It is seen that nitridation of Si causes increase in antimony diffusion. As Sb is believed to diffuse only with the help of vacancies, the increase in Sb diffusion indicates supersaturation of vacancy during the nitridation process. Mizuo and Higuchi [17] first reported the effect of nitridation on dopant diffusion. They reported Sb diffusion

enhancement at 1000 and 1150°C for times up to 4 hours. This diffusion enhancement suggests vacancy supersaturation due to nitridation process. Retarded diffusion of phosphorus and boron were observed at these temperatures confirming vacancy supersaturation.

It is reported that during the nitridation process there is an initial fast nitride film growth regime followed by a slow growth regime. The total nitride film thickness never exceeds 50 Å [18]. During the growth of the nitride film, increased diffusion of Sb is observed. However when the growth of the nitride film is pinned on 50 Å, the increased diffusion of Sb still occurs. If fact when a thermal nitride film is annealed in inert ambient, there is an enhancement of Sb diffusion. When thermal nitride film is removed then Sb diffusivity returns to its inert value [19]. Ahn *et al.* [20] proposed formation of Frenkel defects at the Si/Si_3N_4 interface. These defects absorb Si causing a supersaturation of vacancies in the bulk near the interface. However this theory is not yet well accepted.

Chapter 3

REVIEW OF DIFFUSION STUDIES

As mentioned in the previous chapter point defects play a major role in the diffusion mechanisms. Also, different diffusion mechanisms can be effective for different situations. Thus before going to the details of the model applied in this study, it is important to review previously reported results. As the model applied in this study has parameters like self-diffusivity in Si and Ge, it is important to study the previous studies done to determine Si and Ge self-diffusivity and their behaviors as temperature and Ge fraction are varied. As strain is present in the $Si_{1-x}Ge_x$ in $Si/Si_{1-x}Ge_x/Si$ single quantum well (SQW) structures analyzed in this thesis, it is also important to understand how strain influences self-diffusion of Si and Ge. Additionally, before going through the details of modeling interdiffusion, it is valuable to go through previously reported interdiffusion studies. Different experimental approaches have been used in the literature and these are briefly described in this chapter. Finally, extraction procedures of interdiffusion profiles from previously reported results based on which the modeling in this study was done is described.

3.1 Self-Diffusion in Si, Ge and Si-Ge

Historically, self-diffusion studies of silicon have been carried out with radio active isotopes of silicon. For this purpose, the most commonly used isotope for silicon is the readily available ^{31}Si. However the inherent problem associated with ^{31}Si is its very short life time of about 2.65 hours, and its high self-diffusion activation energy. This limits the use of ^{31}Si in the self-diffusion studies done only at fairly high temperatures (above 1050°C).

To overcome the problem mentioned above with ^{31}Si, Ghoshtagore [21] first diffused stable isotope ^{30}Si which was neutron-activated to ^{31}Si after diffusion annealing. The diffusion profile was extracted using chemical sectioning technique which was not able to give accurate diffusion profiles due to improper subtraction of ^{30}Si from the ^{31}Si. This problem was later avoided by Kalinowski and Seguin [22] where they diffused stable ^{30}Si and determined the diffusion profile by SIMS and measured diffusion coefficient at temperature as low as 855°C. They proposed a single self-diffusion mechanism in Si from temperature as low as 855°C to temperature as high as 1175°C.

Self-diffusion in Ge has been studied by several groups using radioactive isotopes of Ge. These studies report the diffusion mechanisms present in Ge and reported the associated activation energies for the diffusion to occur. Vogel *et al.* [23] studied self-diffusion in intrinsic germanium single crystal for temperatures in the range 549-890°C using ^{71}Ge as an isotope and reported vacancy mechanism for self-diffusion to occur with activation energy of 3.14 ± 0.02 eV. A similar type of study was done by Werner *et al.* [24] where they studied self-diffusion in Ge using ^{71}Ge isotope. The study covered a wide range of temperature, 535-904°C, the range of temperature being similar to the study

done by Vogel *et al.* [23]. Werner *et al.* [24] suggested a vacancy mechanism for self-diffusion in Ge reporting activation energy of 3.09 ± 0.02 eV which is similar to the activation energy values reported by Vogel *et al.* [23]. A similar type of study was done by Campbell [25] where also a single vacancy mechanism was proposed when ^{71}Ge and ^{77}Ge isotopes were used for annealing temperatures at 900 and 925°C. The common features between the findings of all the studies are that the vacancy mechanism is indicated for the self-diffusion process in Ge for all the anneal temperatures.

Seeger and Chik [26] studied Ge diffusion in Si in an early study in 1968, where they first observed a break in Arrhenius behavior of Ge diffusion in Si. They reported that the diffusion takes place by vacancy mechanism at low temperature and by interstitial mechanism at high temperature, the cross over of the mechanisms occurring at 1050°C. Hettich *et al.* [27] studied tracer diffusion of ^{71}Ge and ^{31}Si in intrinsic Si. Ge tracer diffusion in Si was reported for a wide range of temperatures. For diffusion temperatures greater than 1027°C, self-diffusion and germanium diffusion in Si were similar in nature showing very close values of activation energies. Ge tracer diffusion was in fact divided into two regimes, one above 1027°C with high activation energy. In this region the diffusion mechanism was interpreted by interstitial mechanism. Another regime of interest was for diffusion temperatures below 977°C where low value of activation energy was reported. Here diffusion mechanism was interpreted with vacancy mechanism. The results reported by Ogino *et al.* [28] for temperatures in the range 1100-1300°C match well with the results reported by Hettich *et al.* [27]. The high temperature behavior is also supported by studies done by Siethoff and Schroeter [29]. Though a break in Arrhenius behavior was observed by Hettich *et al.* [27], no break was observed by Dorner

et al. [30] in a similar type of study and they reported a single value for activation energy of 5.35 eV for the entire range of temperatures. Similarly no break in Arrhenius behavior was observed by McVay and DuCharme [31].

It is now well accepted that the self-diffusion in Ge in the entire range of diffusion temperature occurs via vacancy mechanism, whereas for self-diffusion in Si and tracer diffusion of Ge in Si, break in the activation energy occurs at around 1050°C. Thus it is of great interest to study Si and Ge diffusion in SiGe materials. It is expected that the diffusion mechanism will depend on the Ge fraction present in SiGe. The study of Ge self-diffusion in SiGe alloys as a fraction of Ge fraction serves to study the difference in self-diffusion mechanism in Si and Ge.

McVay and DuCharme [31] studied the diffusion mechanism of ^{71}Ge in SiGe and reported the variation of activation energy as a function of Ge fraction from pure Si to pure Ge. They reported that activation energy for diffusion remains constant near to 3 eV for Ge fraction from 30% to pure Ge. Below 30%, activation energy rises rapidly up to the value in pure Si. In pure Si, the activation energy was reported to be 5 eV, which is very near to activation energy of Si self-diffusion in pure Si. For a Ge fraction greater than 30% McVay and DuCharme interpreted the diffusion to occur via a vacancy mechanism, whereas for Ge fraction less than 30% the diffusion was interpreted as occurring via an extended defect mechanism. A similar result has been reported by Strohm *et al.* [32] where they studied ^{71}Ge self-diffusion in SiGe as a function of temperature between 894 and 1263°C and as a function of composition from pure Si to pure Ge. The self-diffusivity coefficient was seen to follow an Arrhenius relationship for all the compositions over the temperature range in their study. Activation energies and

pre-exponential factors extracted from the Arrhenius relations show a break at 25% Ge content in SiGe structure. They interpreted this break as the switch from interstitialcy diffusion mechanism on Si side to vacancy mechanism on Ge side.

One of the recent studies on self-diffusion in SiGe was performed by Laitinen *et al.* [33] where they studied self-diffusion of ^{31}Si and ^{71}Ge in relaxed $Si_{0.20}Ge_{0.80}$ in the temperature range 730-950°C. They reported for the first time Si self-diffusion on Si-Ge alloys. According to their study, temperature dependences of the diffusion coefficients for both ^{31}Si and ^{71}Ge followed Arrhenius behavior with activation energy of 3.6 eV and 3.5 eV respectively suggesting vacancy mechanism for diffusion of these elements in $Si_{0.20}Ge_{0.80}$. They also suggested that in $Si_{0.20}Ge_{0.80}$, ^{71}Ge can be used as a substitute for ^{31}Si for self-diffusion studies as both of them diffuse via a vacancy mechanism with very similar activation energies.

Another study was done by Zangenberg *et al.* [34] where they determined activation energies for Ge diffusion in strain-relaxed $Si_{1-x}Ge_x$ with different Ge fraction. For Ge fraction of 0% and 10% they determined an activation energy of 4.7 eV suggesting an interstitial mechanism for diffusion, which decreases to 3.7-4.0 eV for Ge fraction of 20% and 40% suggesting absence of diffusion via vacancies and for Ge fraction of 50% the activation energy were reported 3.2eV. They also measured the effect of strain on Ge self-diffusion in $Si_{1-x}Ge_x$ for temperature range of 925-1050°C and reported decrease in diffusion coefficient from compressive to tensile strain.

Based on the above reported previous results, it can be concluded that Ge fraction in SiGe has a vital role behind the self-diffusion mechanism in SiGe. Self-diffusion is reported to occur by interstitial mechanism at Si side which is switched to vacancy

mechanism at Ge side of SiGe material depending on the Ge fraction present on the material.

3.2 Interdiffusion Studies of $Si_{1-x}Ge_x$/Si Heterostructures

Several groups have attempted to characterize interdiffusion in $Si_{1-x}Ge_x$/Si structures, with different experimental methods followed in the different studies.

Photoluminescence (PL) is reported to be a powerful technique to detect interdiffusion as reported by Sunamura *et al.* [35]. The study was performed on $Si_{1-x}Ge_x$/Si quantum wells (QW) grown by gas source molecular beam epitaxy. They did not consider the dependence of interdiffusion of Si and Ge in the structure to the variation of Ge content and determined only the effective numbers for interdiffusion for different cases. The samples were annealed in vacuum for 20 min at temperatures ranging 800-950°C. The diffusivities were calculated from the luminescent peak energy blue shifts by the method described in ref. [36]. The diffusivities were reported to follow Arrhenius behavior with activation energy of around 3 eV.

Another technique adopted to determine the interdiffusion coefficient is Rutherford Backscattering (RBS). Strain and concentration independent interdiffusion coefficient from Ge profiles determined by RBS in Si/$Si_{1-x}Ge_x$/Si structures was reported by Ijzendoorn *et al.* [37]. The determined coefficients show Arrhenius behavior and agree remarkably with the results for Ge tracers in Si reported previously [38]. They also reported increase in Ge interdiffusion with the increase in Ge content in the structure. The influence of strain to the interdiffusion along with the influence of the variation of Ge content was studied by Holländer *et al.* [39]. They reported effective interdiffusivity values both in symmetrically and asymmetrically strained $Si_{1-x}Ge_x$/Si superlattices

measured by RBS in the temperature range between 900 and 1125°C. The effect of strain on interdiffusivity was reported to be small and the interdiffusivity was reported to be increased for higher Ge concentration in the structure as was reported by Ijzendoorn *et al.* [37]. The temperature dependence of interdiffusivity coefficients for a given Ge content was reported to follow Arrhenius behavior for all the cases with activation energies around 4 eV.

X-Ray Diffraction (XRD) is another method applied to determine interdiffusivity which offers much higher sensitivity in measuring diffusion compared to other techniques. Baribeau *et al.* [40] reported effective interdiffusivity in $(Si_mGe_n)_p$ superlattice structure using XRD where they observed a strong interdiffusion enhancement in the early stages of annealing of the samples. This behavior was correlated with the high initial strain present in the structure which disappears upon relaxation of the structure during annealing. The reported interdiffusivity values showed Arrhenius behavior. They observed higher interdiffusion for structures having thick Ge and thin Si layers. However, no definite mechanism for the interdiffusion to occur was proposed in the study. On the other hand using XRD technique Chang *et al.* [41] proposed a mono vacancy diffusion mechanism for interdiffusion in a symmetrically strained Ge/Si superlattice consisting of alternative Si and Ge layers grown on $Si_{0.6}Ge_{0.4}$ buffer layer for annealing in the temperature range 640-780°C. The calculated interdiffusivity coefficients were reported to follow Arrhenius behavior with activation energy of 3.1 ± 0.2 eV. The interdiffusion behavior in long-period $Si_{0.7}Ge_{0.3}$/Si superlattice structure using XRD and Raman spectroscopy was studied by Prokes *et al.* [42]. They reported interdiffusion activation energies in symmetrically and

asymmetrically grown structures to be 3.9 and 4.6 eV respectively. They observed enhancement in interdiffusion under external tensile stress applied to asymmetrically strained superlattice structure.

To quantify Ge interdiffusion in $Si/Si_{0.85}Ge_{0.15}/Si$, studies were done by Griglione *et al.* [43]-[44]. The samples were annealed in inert and oxidizing ambients in temperature range 900-1200°C and for nitriding ambient in temperature range 1100-1200°C for different anneal times. For inert and oxidizing ambients they suggested a vacancy exchange mechanism for interdiffusion to occur for the entire range of temperatures with activation energies 5.8 and 5.0 eV respectively. These values of activation energies are however much higher than the corresponding values reported by others for vacancy exchange mechanism to dominate for the interdiffusion phenomena. For nitriding ambient minimal vacancy contribution in the interdiffusion phenomena was reported which contradicts with the findings in inert and oxidizing ambient studies for the samples annealed in the same temperature range.

One interesting study was done by Iyer and LeGoues [45] where they reported the relation between the strain and interdiffusion phenomena in $Si_{0.88}Ge_{0.12}/Si$ superlattice structure. They reported that interdiffusion occurred for the structures which were initially free of misfit dislocations and the structures were relieved from initial strain through interdiffusion. For superlattice structures where initial misfit dislocations were present, the structures were relaxed by dislocation multiplication process and negligible amount of interdiffusion phenomena were observed in the structures.

Interdiffusion studies have so far been performed on different types of structures and attempts were taken to observe interdiffusion phenomena using different measurement techniques. The results of studies done by different groups agree that increased interdiffusivity is observed with the increase in Ge content. Also most of the studies agree interdiffusion measured with varying temperatures show Arrhenius behavior though agreement between the activation energies from one group to other are rarely observed. Though several techniques have been applied to quantify the interdiffusion in different structures, yet no modeling is attempted to perform to describe the interdiffusion behavior. To understand the interdiffusion mechanism properly it is important to do atomistic modeling of this phenomenon, which is in fact the subject of this thesis.

3.3 Extraction of Experimental Profiles

For the modeling of Si and Ge interdiffusion mechanism done in this study, previously reported results reported by Griglione *et al.* [43]-[44] and Ijzendoorn *et al.* [37] were taken as reference. The main conclusions done by these studies are mentioned in the previous section. These studies facilitates with experimental results using which it was possible extract experimental Ge interdiffusion profiles in the studied structures. Once the experimental profiles were extracted, the modeling was performed on those profiles. At Sections 3.3.1 and 3.3.2, the details of the extraction of the experimental Ge interdiffusion profiles are described.

3.3.1 The Experiment by Griglione *et al.*

A SQW $Si/Si_{0.85}Ge_{0.15}/Si$ structure was taken a reference for modeling interdiffusion mechanism of Si and Ge. The reference sample contained 50 nm undoped Si cap, followed by 50 nm thick undoped $Si_{0.85}Ge_{0.15}$ layer which was followed by 100 nm thick undoped Si buffer layer and lightly *p*-doped Si substrate as shown in Figure 3.1. The samples were grown and studied by Griglione *et al.* [43]-[44]. They used Molecular Beam Epitaxy (MBE) [46] to grow the samples at a temperature of 520°C. The samples were thoroughly characterized for Ge concentration, Ge profile, layer depth and the presence of extended defects. The details of sample growth, annealing in inert, oxidizing and nitriding ambients and the characterization techniques can be found from ref. [47].

The annealing conditions for the samples are summarized in Table 3.1. Effective diffusivities for Ge interdiffusion in the structure for all these different anneal conditions were reported by Griglione [47]. Griglione extracted the effective diffusivities for all the cases using the non-commercial version of the process simulator FLOOPS. The reported

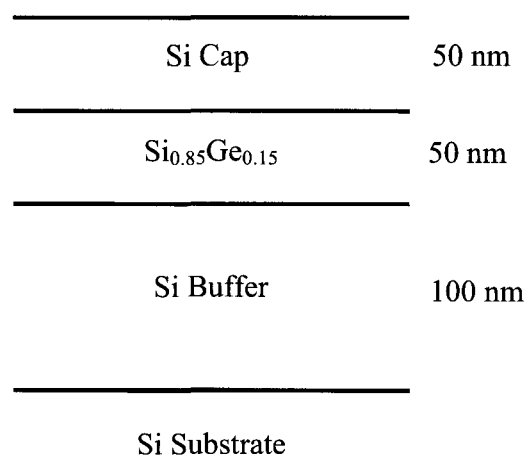

Figure 3.1: Sample $Si/Si_{0.85}Ge_{0.15}/Si$ SQW structure.

Temperature (°C)	Anneal times in inert ambient (min)	Anneal times in oxidizing ambient (min)	Anneal times in nitriding ambient (min)
900	330	330	
	980		
	1532		-
	2206		
1000	43	43	
	55	55	-
	87	87	
	125	125	
1100	1	1	1
	2	2	2
	3	3	3
	4	4	4
1200	1	1	1
	1.5	1.5	1.5
	2	2	2
	3	3	3

Table 3.1: Anneal conditions for the samples studied by Griglione *et al.* [43]-[44].

effective diffusivities were extracted from reasonable fits to the experimental secondary ion mass spectrometry (SIMS) [48] profiles. During the extraction process of effective diffusivity, *Fermi* diffusion model of FLOOPS was used. *Fermi* model assumes that the point defects remain in equilibrium and the point defect equations are not solved. Thus using *Fermi* model in the extraction process gives an idea of how Ge interdiffusion behaves with the annealing along with the change in ambients, and yields an overall effective diffusivity without delving into the atomistic diffusion mechanism.

In this study using these extracted effective diffusivities by Griglione *et al.* [43]-[44], the experimental concentration profiles were obtained by diffusing the as-grown Ge profiles using these constant diffusivities for the specified anneal times. We used

FLOOPS-ISE, the commercial version of FLOOPS to extract the experimental Ge interdiffusion profiles from the effective diffusivities reported by Griglione *et al.*. The same *Fermi* model was used to extract the experimental profiles.

In the cases where the actual experimental profiles were available, we compared our extracted profiles with the experimental profiles. It was found that the extracted Ge interdiffusion profiles matched very well with the experimental SIMS profiles for all the cases. This ensures that the extracted Ge interdiffusion profiles in fact represent very well the actual experimental Ge interdiffusion profiles. Figure 3.2 shows a match between the extracted annealed Ge interdiffusion profile with the experimental SIMS profile for sample annealed in inert ambient at 1000°C for 43 min. The extracted profile matches very well with the experimental profile.

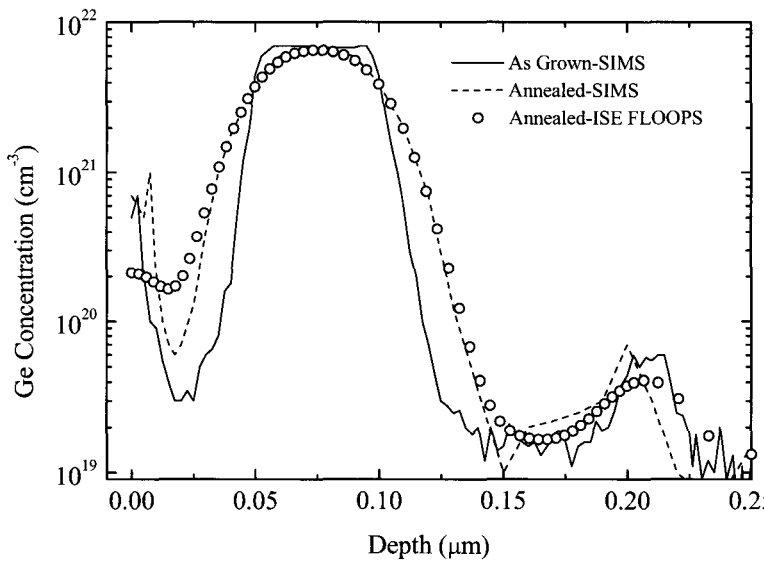

Figure 3.2: Match between the extracted experimental profile and the experimental SIMS profile for sample annealed in inert ambient at 1000°C for 43 min.

Similar match was observed for the sample annealed in nitriding ambient at 1100°C for 3 min as shown in Figure 3.3. In the remainder of this thesis, the extracted Ge interdiffusion profiles thus determined will be referred to as extracted experimental Ge interdiffusion profiles.

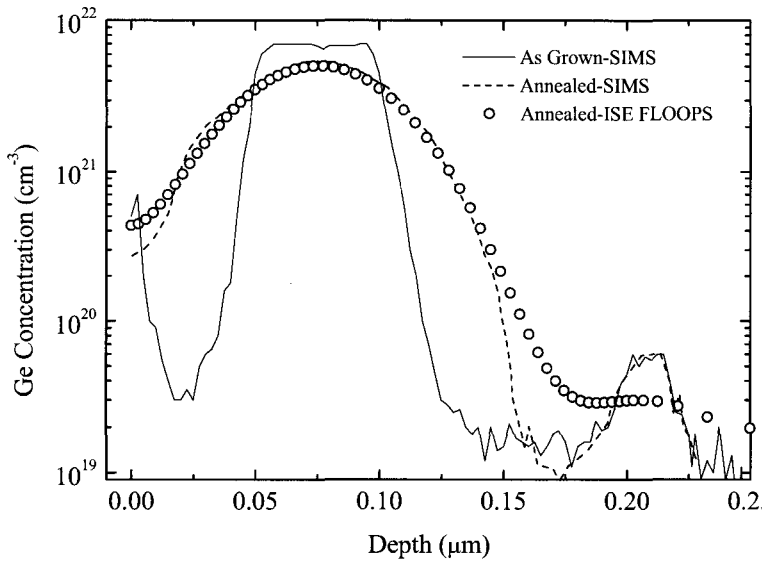

Figure 3.3: Match between the extracted experimental profile and the experimental SIMS profile for sample annealed in nitriding ambient at 1100°C for 3 min.

Sample code for extracting the experimental profiles in the above mentioned ways is provided in Appendix A.1.

3.3.2 The Experiment by Ijzendoorn *et al.*

Ijzendoorn *et al.* [37] reported Ge interdiffusion profiles for $Si/Si_{0.83}Ge_{0.17}/Si$ SQW samples annealed in inert ambient at 970°C for 5, 15, 30 and 60 min. They used RBS technique [49] to measure the as-grown Ge profile and the Ge interdiffusion profiles after the annealing. The samples were grown by MBE technique, the grown samples had

similar structures compared to the samples studied by Griglione *et al.* [43]-[44], the only difference was Griglione *et al.* used $Si_{1-x}Ge_x$ layers containing 15% Ge whereas Ijzendoorn *et al.* used $Si_{1-x}Ge_x$ layers containing 17% Ge. Ijzendoorn *et al.* [37] reported RBS profiles for Ge interdiffusion after annealing was performed. We extracted the Ge concentration as a function of sample depth from those reported RBS profiles. As the normalized yields of RBS profile are proportional to the Ge concentrations, the highest normalized yield of RBS profile was for 17% Ge, and considering this the normalized yields were converted to Ge concentrations in cm^{-3}. Again the width of the RBS profile is related to the actual width of the studied material, and there was a marker indication for the starting point of the SiGe layer. Based on these, the RBS energies were converted to sample depth and finally concentration of Ge as a function of depth in the sample was extracted.

The extracted profiles were used for the modeling purposes based on the model developed in Chapter 4. Finally the simulation results based on the modeling are provided in Chapter 5.

Chapter 4

MATHEMATICAL MODEL FOR Si/Ge INTERDIFFUSION

In the SiGe alloy, the Si and Ge atoms may either occupy a substitutional site or an interstitial site. The substitutional atom may only move by exchange with an adjacent vacancy. This is known as vacancy exchange mechanism. The interstitial atom moves by hopping from one interstitial site to an adjacent one. The exchange between substitutional and interstitial atoms may occur by a kick out reaction, where one of the two atoms is a Si atom and the other is a Ge atom, or by a bulk generation-recombination reaction where a single species switch from the substitutional to the interstitial or vice versa. This chapter considers each of these reactions and formulates a system of equations that describe these diffusion processes. The vacancy exchange mechanism is considered first, then the interstitial component is taken into account.

4.1 Model for Vacancy Exchange Mechanism

One of the simplest mechanisms for atoms to diffuse is the vacancy exchange mechanism. For temperatures below 1050°C, self-diffusion of Si in pure Si occurs by the vacancy exchange mechanism. However, above this temperature the self-diffusion is

thought to occur by an interstitial mechanism. On the other hand self-diffusion of Ge in pure Ge is reported to occur only by the vacancy exchange mechanism at all temperatures. Thus it is of interest to see how interdiffusion of Si and Ge in $Si/Si_{1-x}Ge_x/Si$ single quantum well (SQW) structure occurs in a wide range of temperatures.

The vacancy exchange mechanism was first proposed by Kirkendall *et al.* [50] to interpret interdiffusion in metallic systems. Detailed mathematical formulations were developed by Smigelskas and Kirkendall [51] and Darken [52]. The model is based on the observation that a substitutional atom will diffuse only if its adjacent site is vacant. The substitutional atom and the vacancy interchange their positions with each other and one step of the diffusion occurs. In semiconductors, vacancies may deviate from their equilibrium concentration. A modification for the model to take this into account was proposed by Tai [53] and Chase *et al.* [54]. Here, a further modification is considered to take into account the case where the equilibrium vacancy concentration is not constant in space. The mathematical model to describe this mechanism arises from the following argument. Consider a very simple situation with only two atomic planes at x and $x + \Delta x$ as shown in Figure 4.1. The atomic planes are separated by the lattice spacing, Δx. An atom at plane x jumps to the other atomic plane if a vacancy is present there. Similarly an atom at position $x + \Delta x$ will jump to the other plane if the other plane holds a vacancy.

Let the number of atoms per unit volume be denoted by C_A and the number of vacancies per unit volume is C_V.

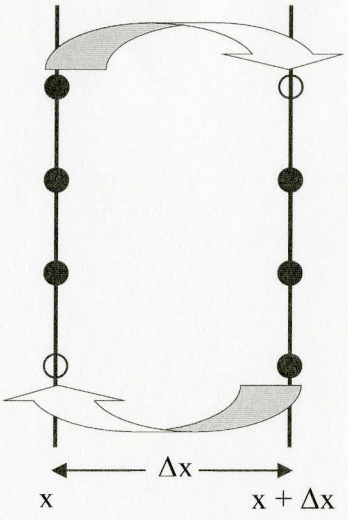

Figure 4.1: Basic diagram for vacancy exchange mechanism.

Thus,

The number of atoms per unit area, $N_A = C_A \,.\, \Delta x$

and the number of vacancies per unit area, $N_V = C_V \,.\, \Delta x$

We argue that the rate of a jump from a plane is proportional to the concentration of atoms at that plane and the concentration of vacancies on the other plane *normalized* to its equilibrium value. Hence, the flux of diffusing atoms from plane x to plane x + Δx,

$$J_1 = \delta(x).C_A(x).\Delta x.\frac{C_V(x+\Delta x).\Delta x}{C_V^*(x+\Delta x).\Delta x}$$

$$\text{or, } J_1 = \delta(x).C_A(x).\Delta x.\frac{C_V(x+\Delta x)}{C_V^*(x+\Delta x)} \qquad \textbf{(4.1)}$$

Here δ is the probability of an atom jump from one atomic plane to another atomic plane and C_V^* is the equilibrium vacancy concentration.

Similarly, the flux of diffusing atoms from plane x + Δx to plane x,

$$J_2 = \delta(x+\Delta x).C_A(x+\Delta x).\Delta x.\frac{C_V(x)}{C_V^*(x)} \tag{4.2}$$

Thus the net flux for diffusion,

$$J = J_1 - J_2 = \Delta x.\left[\delta(x).C_A(x).\frac{C_V(x+\Delta x)}{C_V^*(x+\Delta x)} - \delta(x+\Delta x).C_A(x+\Delta x).\frac{C_V(x)}{C_V^*(x)}\right]$$

$$= \Delta x.\left[\delta(x).C_A(x).\frac{C_V(x)}{C_V^*(x)} + \Delta x.\delta(x).C_A(x).\frac{\partial}{\partial x}\left\{\frac{C_V(x)}{C_V^*(x)}\right\} - \delta(x).C_A(x).\frac{C_V(x)}{C_V^*(x)}\right.$$

$$\left. - \Delta x.\frac{\partial}{\partial x}\{\delta(x).C_A(x)\}.\frac{C_V(x)}{C_V^*(x)}\right]$$

$$\text{or, } J = (\Delta x)^2\left[\delta(x).C_A(x).\frac{\partial}{\partial x}\left\{\frac{C_V(x)}{C_V^*(x)}\right\} - \delta(x).\frac{C_V(x)}{C_V^*(x)}.\frac{\partial C_A(x)}{\partial x}\right] \tag{4.3}$$

Where a Taylor's expansion was used for the quantities at position x + Δx, and it is assumed that the atom jump frequency is independent of concentration.

Since the atom jump frequency is assumed independent of concentration, it may be set to its value under intrinsic conditions. Then, from equation (4.3) the net flux for diffusion becomes,

$$J = (\Delta x)^2\left[\delta^*(x).C_A(x).\frac{\partial}{\partial x}\left\{\frac{C_V(x)}{C_V^*(x)}\right\} - \delta^*(x).\frac{C_V(x)}{C_V^*(x)}.\frac{\partial C_A(x)}{\partial x}\right] \tag{4.4}$$

Here $\delta^*(x)$ represents the probability of an atom jump from plane x under inert intrinsic conditions and C_V^* represent intrinsic equilibrium vacancy concentration.

Now define the diffusivity at inert intrinsic condition as,

$$D_A^* = \delta^*.(\Delta x)^2 \tag{4.5}$$

Thus using equation (4.5) in equation (4.4) the expression of net flux of diffusion becomes,

$$J = D_A^*.C_A.\frac{\partial}{\partial x}\left(\frac{C_V}{C_V^*}\right) - D_A^*.\frac{C_V}{C_V^*}.\frac{\partial C_A}{\partial x} \tag{4.6}$$

Equation (4.6) represents the basic equation for interdiffusion flux in a system. Based on this equation the interdiffusion fluxes of Si and Ge in $Si/Si_{1-x}Ge_x/Si$ SQW structure can be represented as follows.

The interdiffusing flux for Ge is,

$$J_{Ge} = D_{Ge}^*.C_{Ge}.\frac{\partial}{\partial x}\left(\frac{C_V}{C_V^*}\right) - D_{Ge}^*.\frac{C_V}{C_V^*}\frac{\partial C_{Ge}}{\partial x} \tag{4.7}$$

And the interdiffusing flux for Si is,

$$J_{Si} = D_{Si}^*.C_{Si}.\frac{\partial}{\partial x}\left(\frac{C_V}{C_V^*}\right) - D_{Si}^*.\frac{C_V}{C_V^*}\frac{\partial C_{Si}}{\partial x} \tag{4.8}$$

Conversation of lattice site density requires,

$$J_{Ge} + J_{Si} + J_V = 0 \tag{4.9}$$

so that

$$J_V = -\left[D_{Ge}^*.C_{Ge}.\frac{\partial}{\partial x}\left(\frac{C_V}{C_V^*}\right) - D_{Ge}^*.\frac{C_V}{C_V^*}\frac{\partial C_{Ge}}{\partial x} + D_{Si}^*.C_{Si}.\frac{\partial}{\partial x}\left(\frac{C_V}{C_V^*}\right) - D_{Si}^*.\frac{C_V}{C_V^*}\frac{\partial C_{Si}}{\partial x}\right] \tag{4.10}$$

Based on these flux equations for Ge, Si and vacancy represented by equations (4.7), (4.8) and (4.10) respectively; the continuity equations for Ge, Si and vacancy can be represented respectively by equations (4.11), (4.12) and (4.13).

$$\frac{\partial C_{Ge}}{\partial t} = -\frac{\partial}{\partial x}\left[D_{Ge}^*.C_{Ge}.\frac{\partial}{\partial x}\left(\frac{C_V}{C_V^*}\right) - D_{Ge}^*.\frac{C_V}{C_V^*}\frac{\partial C_{Ge}}{\partial x}\right] \tag{4.11}$$

$$\frac{\partial C_{Si}}{\partial t} = -\frac{\partial}{\partial x}\left[D^{*}_{Si}.C_{Si}.\frac{\partial}{\partial x}\left(\frac{C_V}{C^{*}_V}\right) - D^{*}_{Si}.\frac{C_V}{C^{*}_V}\frac{\partial C_{Si}}{\partial x}\right] \tag{4.12}$$

$$\frac{\partial C_V}{\partial t} = \frac{\partial}{\partial x}\left[D^{*}_{Ge}.C_{Ge}.\frac{\partial}{\partial x}\left(\frac{C_V}{C^{*}_V}\right) - D^{*}_{Ge}.\frac{C_V}{C^{*}_V}\frac{\partial C_{Ge}}{\partial x} + D^{*}_{Si}.C_{Si}.\frac{\partial}{\partial x}\left(\frac{C_V}{C^{*}_V}\right) - D^{*}_{Si}.\frac{C_V}{C^{*}_V}\frac{\partial C_{Si}}{\partial x}\right] \tag{4.13}$$

Here C_{Ge}, C_{Si} and C_V are respectively the concentrations of Ge, Si and vacancy.

4.2 Modeling the Interstitial Contribution

The vacancy exchange mechanism might not satisfy all the interdiffusion cases. Thus it is also important to consider the role of interstitials in interdiffusion along with the vacancy exchange mechanism. The role of interstitials is taken into account by considering two mechanisms: the kick-out (KO) mechanism and the bulk recombination (R) mechanism.

In KO mechanism, an interstitial atom of one species (Si or Ge) kicks out a substitutional atom of the other species. The process is shown by the following relation.

$$Ge_S + Si_I \Leftrightarrow Si_S + Ge_I \tag{4.14}$$

The subscripts S and I respectively represents whether atoms resides at substitutional or interstitial site. The forward and reverse reaction rates are referred respectively as $k_{f,KO}$ and $k_{r,KO}$.

Also the interstitial Ge and Si can recombine with vacancies and become substitutional Ge and Si respectively by a bulk recombination process as shown by the following relations.

$$V + Si_I \Leftrightarrow Si_S \tag{4.15}$$

$$V + Ge_I \Leftrightarrow Ge_S \tag{4.16}$$

The forward and reverse reaction rate constants for Si recombination process respectively are referred as $k_{f,SiR}$ and $k_{r,SiR}$, the forward and reverse reaction rate constants for Ge recombination process respectively are referred as $k_{f,GeR}$ and $k_{r,GeR}$.

The concentrations of Ge_S, Ge_I, Si_S, Si_I, and V are respectively represented as C_{Ge_S}, C_{Ge_I}, C_{Si_S}, C_{Si_I} and C_V.

Before going to the details of the equations describing the diffusion process, it is important to understand each of the reaction parameters mentioned above. Under diffusion limited conditions, the forward reaction rate constant $k_{f,KO}$ can be expressed as [55],

$$k_{f,KO} = 4.\pi.r_{Si}.D_{Si_I} \tag{4.17}$$

where, r_{Si} is the capture radius of a Si interstitial by a Ge substitutional and D_{Si_I} is the diffusivity of interstitial Si.

Similarly, $k_{r,KO}$ can be expressed as,

$$k_{r,KO} = 4.\pi.r_{Ge}.D_{Ge_I} \tag{4.18}$$

where, r_{Ge} is the capture radius of a Ge interstitial by a Si substitutional and D_{Ge_I} is the diffusivity of interstitial Ge.

Again, under diffusion limited condition $k_{f,SiR}$ can be expressed as [55],

$$k_{f,SiR} = 4.\pi.r_{IVSi}.(D_{Si_I} + D_V) \tag{4.19}$$

Similarly,

$$k_{f,GeR} = 4.\pi.r_{IVGe}.(D_{Ge_I} + D_V) \tag{4.20}$$

Here, D_V is the diffusivity of vacancy itself, r_{IVGe} and r_{IVSi} respectively are the recombination radii for Ge and Si.

When the Si recombination reaction is at equilibrium we may write,

$$k_{f,SiR}.C^*_{Si_I}.C^*_V = k_{r,SiR}.C_{Si_S} \tag{4.21}$$

Similarly,

$$k_{f,GeR}.C^*_{Ge_I}.C^*_V = k_{r,GeR}.C_{Ge_S} \tag{4.22}$$

where the superscript '*' represents the equilibrium state of the corresponding parameter.

Thus for reactions (4.15) and (4.16) the net fluxes to the right may be written as,

$$k_{f,SiR}.C_{Si_I}.C_V - k_{r,SiR}.C_{Si_S} = k_{f,SiR}(C_{Si_I}.C_V - C^*_{Si_I}.C^*_V) \tag{4.23}$$

$$k_{f,GeR}.C_{Ge_I}.C_V - k_{r,GeR}.C_{Ge_S} = k_{f,GeR}(C_{Ge_I}.C_V - C^*_{Ge_I}.C^*_V) \tag{4.24}$$

Based on the above discussions and calculations, it is possible to write continuity equations for all the species in the system. For this situation we have to consider five species: the substitutional Ge (Ge_S), the substitutional Si (Si_S), the interstitial Ge (Ge_I), the interstitial Si (Si_I), and the vacancy (V). The continuity equations for the complete system can be written as follows:

$$\frac{\partial C_{Ge_S}}{\partial t} = \frac{\partial}{\partial x}\left\{D^*_{Ge}.\frac{C_V}{C^*_V}.\frac{\partial C_{Ge_S}}{\partial x} - D^*_{Ge}.C_{Ge_S}.\frac{\partial}{\partial x}\left(\frac{C_V}{C^*_V}\right)\right\} - k_{f,KO}.C_{Ge_S}.C_{Si_I} + k_{r,KO}.C_{Si_S}.C_{Ge_I}$$
$$+ k_{f,GeR}(C_{Ge_I}.C_V - C^*_{Ge_I}.C^*_V) \tag{4.25}$$

$$\frac{\partial C_{Si_S}}{\partial t} = \frac{\partial}{\partial x}\left\{D^*_{Si}.\frac{C_V}{C^*_V}.\frac{\partial C_{Si_S}}{\partial x} - D^*_{Si}.C_{Si_S}.\frac{\partial}{\partial x}\left(\frac{C_V}{C^*_V}\right)\right\} + k_{f,KO}.C_{Ge_S}.C_{Si_I} - k_{r,KO}.C_{Si_S}.C_{Ge_I}$$
$$+ k_{f,SiR}(C_{Si_I}.C_V - C^*_{Si_I}.C^*_V) \tag{4.26}$$

$$\frac{\partial C_{Ge_I}}{\partial t} = \frac{\partial}{\partial x}\left\{D_{Ge_I}.C^*_{Ge_I}.\frac{\partial}{\partial x}\left(\frac{C_{Ge_I}}{C^*_{Ge_I}}\right)\right\} + k_{f,KO}.C_{Ge_S}.C_{Si_I} - k_{r,KO}.C_{Si_S}.C_{Ge_I} - k_{f,GeR}(C_{Ge_I}.C_V - C^*_{Ge_I}.C^*_V)$$

(4.27)

$$\frac{\partial C_{Si_I}}{\partial t} = \frac{\partial}{\partial x}\left\{ D_{Si_I}.C^*_{Si_I}.\frac{\partial}{\partial x}\left(\frac{C_{Si_I}}{C^*_{Si_I}}\right)\right\} - k_{f,KO}.C_{Ge_S}.C_{Si_I} + k_{r,KO}.C_{Si_S}.C_{Ge_I} - k_{f,SiR}(C_{Si_I}.C_V - C^*_{Si_I}.C^*_V)$$

(4.28)

Finally, considering lattice site conservation requires:

$$C_{Ge_S} + C_{Si_S} + C_V = constant \qquad \textbf{(4.29)}$$

Thus based on the above relation, it is possible to write the continuity equation for the vacancy as:

$$\frac{\partial C_V}{\partial t} = -\frac{\partial C_{Ge_S}}{\partial t} - \frac{\partial C_{Si_S}}{\partial t}$$

$$= \frac{\partial}{\partial x}\left\{ D^*_{Ge}.C_{Ge_S}.\frac{\partial}{\partial x}\left(\frac{C_V}{C^*_V}\right) - D^*_{Ge}.\frac{C_V}{C^*_V}.\frac{\partial C_{Ge_S}}{\partial x} + D^*_{Si}.C_{Si_S}.\frac{\partial}{\partial x}\left(\frac{C_V}{C^*_V}\right) - D^*_{Si}.\frac{C_V}{C^*_V}.\frac{\partial C_{Si_S}}{\partial x}\right\}$$

$$- k_{f,GeR}(C_{Ge_I}.C_V - C^*_{Ge_I}.C^*_V) - k_{f,SiR}(C_{Si_I}.C_V - C^*_{Si_I}.C^*_V) \qquad \textbf{(4.30)}$$

The five continuity equations given above describe the complete system taking into account the motion of both substitutional and interstitial atoms, and the interaction between different species in the system. In Chapter 5 we consider the experimental data in light of the different components of this model.

Chapter 5

RESULTS AND DISCUSSIONS

5.1 Simulation Approach

In this study, the Alagator Scripting Language tool of FLOOPS-ISE was extensively used. The experimentally grown structure which was considered as a reference work for this study was defined using FLOOPS-ISE. The mathematical equations derived in Chapter 4 were then applied using Alagator Scripting Language feature. Sample codes illustrating the implementation of the various terms in the equations are provided in the Appendix A.

For simulating any model using FLOOPS-ISE it is necessary to initialize all the diffusing elements with the appropriate initial conditions. Also it is necessary to define appropriate boundary conditions for the structure. For vacancy exchange mechanism there are three species that needed to be considered. These are substitutional Si (Si_S), substitutional Ge (Ge_S), and vacancy (Vac). Also the recombination of Vac with Si interstitials (Si_I) are considered. Thus the only role of Si_I while applying the vacancy flux model is its recombination with Vac and thus a recombination term of Vac with Si_I is

included with the vacancy equation of the vacancy flux model. To include the effect of recombination of *Vac* with Si_I, the recombination term *Kbulk*(Vac* Si_I-EqVac*EqSi$_I$)* was added to the vacancy equation of the vacancy flux model. *Kbulk* refers to the bulk recombination coefficient of *Vac* and Si_I and *EqVac* and *EqSi*$_I$ respectively are the equilibrium values of *Vac* and Si_I. For Si_I, the default model in FLOOPS-ISE was considered.

As there are four species, four equations are needed to completely describe the system. A continuity equation for each of these elements can be used and the complete system can be defined. However there is an equation describing the conservation of lattice sites which is,

$$C_{Si} + C_{Ge} + C_V = Constant \tag{5.1}$$

Here, C_{Si}, C_{Ge} and C_V respectively are the concentrations of Si, Ge and vacancy.

Using this lattice site conservation constraint it is possible to eliminate one of the continuity equations. As Si_S is the most abundantly available species, computationally it is most difficult to determine and thus it is logical to replace the continuity equation of Si_S with the conservation of lattice site constraint. Finally there are three continuity equations along with an equation for conservation of lattice sites. For interstitial Si and vacancy, the natural boundary condition defined in FLOOPS-ISE was applied at the top surface.

When the effects of interstitials are considered along with the vacancy exchange mechanism, there are five species present in the system, which are, substitutional Si (Si_S), substitutional Ge (Ge_S), interstitial Si (Si_I), interstitial Ge (Ge_I) and vacancy (*Vac*). For this case the five continuity equations described in Charter 4 can be applied to describe the total system. However the conservation of lattice sites facilitates replacing the

continuity equation of Si_S with the equation of conservation of lattice sites in this case too. Ultimately the total system can be described with four continuity equations and an equation for conservation of lattice sites. For this case natural boundary condition defined in FLOOPS-ISE was applied for interstitial Si and vacancy at the top surface of the structure.

When applying only the vacancy exchange mechanism, the fitting parameters for the simulations were intrinsic self-diffusivities of Ge and Si (D^*_{Ge} and D^*_{Si}). The initial profile for intrinsic equilibrium vacancy concentration (C^*_V) were also varied as a function of Ge fraction in the structure. For the diffusivities, values have been reported in the literature as discussed in Chapter 3. For C^*_V we believe that it should be higher in SiGe than in Si. However, the comparative magnitudes are not well established. Considering C^*_V to be constant throughout the profile, and constraining the diffusivities to be close to their published values we were able to fit the low temperature data as discussed in detail later in this chapter. We then experimented with the effect of increasing C^*_V in the SiGe layer and thus obtained an upper bound on C^*_V for SiGe. The fitting parameters were optimized to produce the best overall match between simulation and experiment using the same values of the parameters for all anneal times at a given temperature. The sample codes applied using FLOOPS-ISE when only the vacancy exchange model was considered is given in Appendix A.2.

When the effects of interstitials were considered along with the vacancy exchange mechanism, the fitting parameters used for the simulations were intrinsic self-diffusivities of Ge and Si (D^*_{Ge} and D^*_{Si}), diffusivity of interstitial Si (D_{Si_I}), diffusivity of interstitial

Ge (D_{Ge_I}) and equilibrium concentrations of Si and Ge interstitials as well as vacancy. All these fitting parameters were fixed in such a way that for each anneal temperature keeping the parameters fixed, the simulated Ge profiles showed good match with the extracted experimental Ge interdiffusion profiles for all anneal times at that particular temperature. The fitting parameters used in the modeling are compared with the previously reported values to justify the validity of the model. The sample FLOOPS-ISE codes used in the simulations when the effects of interstitials were considered along with the vacancy exchange model is given in Appendix A.3.

For simulations in oxidizing ambient, the oxidation model of FLOOPS-ISE was used to oxidize the capping Si layer of the structure during the simulations. This included a default level of interstitial injection during the oxidation.

It is well accepted that vacancies are injected during nitridation of Si. In FLOOPS-ISE, no default model for injection of vacancies during nitridation of Si is provided. Thus, to model Ge interdiffusion in nitriding ambient, it was necessary to model injection of vacancies along with the interdiffusion modeling. To model the vacancy injection, previously reported results on Sb diffusion in Si were used. The details of the vacancy injection modeling steps are described in Section 5.3.2. The FLOOPS-ISE samples codes to set vacancy injection parameters are provided in Appendix A.4.

5.2 Interdiffusion at Temperatures Below 1050°C

Below 1050°C the self-diffusion of both Si and Ge is dominated by the vacancy mechanism. Hence, it is reasonable to expect that in this temperature regime the interdiffusion would also be dominated by a vacancy mechanism. Griglione *et al.* [43] performed anneals at 900 and 1000°C in inert and oxidizing ambients as summarized in

Table 3.1 and Ijzendoorn *et al.* [37] performed anneals at 970°C for 5, 15, 30 and 60 min in inert ambient.

We followed the simulation approach outlined in Section 5.1. The initial profile for Ge was set to be the same as the as-grown SIMS profile determined from experimental studies. First, the model was applied for samples annealed in inert ambient. Intrinsic self-diffusivities of Ge and Si (D^*_{Ge} and D^*_{Si}) were varied as a function of Ge fraction in the structure and these were used as fitting parameters. The parameters were optimized so that at a given temperature the same diffusivities were used for all anneal times. Figure 5.1 shows the comparison between experimental and simulated Ge interdiffusion profiles in inert ambient at 900°C for 330 min and 2206 min anneal times. Figure 5.2 shows the fits for 970°C for 30 min and 60 min. Figure 5.3 shows the comparison between experimental and simulated Ge interdiffusion profiles in inert ambient at 1000°C for 43 min and 125 min anneal times.

With good fits for the inert case, the oxidizing ambient anneals at 900 and 1000°C were simulated in the same manner. The default FLOOPS-ISE oxidation model and interstitial injection model during Si oxidation were used. For 900°C, only the 330 min anneal was considered. For higher anneal times the total Si capping layer was consumed during oxidation and the $Si_{1-x}Ge_x$ layer partially oxidized. The injection of point defects during $Si_{1-x}Ge_x$ oxidation has yet to be studied in detail. Hence we elected not to attempt a model of the longer anneal times. As no well accepted oxidation model is available for $Si_{1-x}Ge_x$ oxidation, simulations at anneal temperatures above 330 min were not performed. Typical fits are shown in Figure 5.4, Figure 5.5 and Figure 5.6.

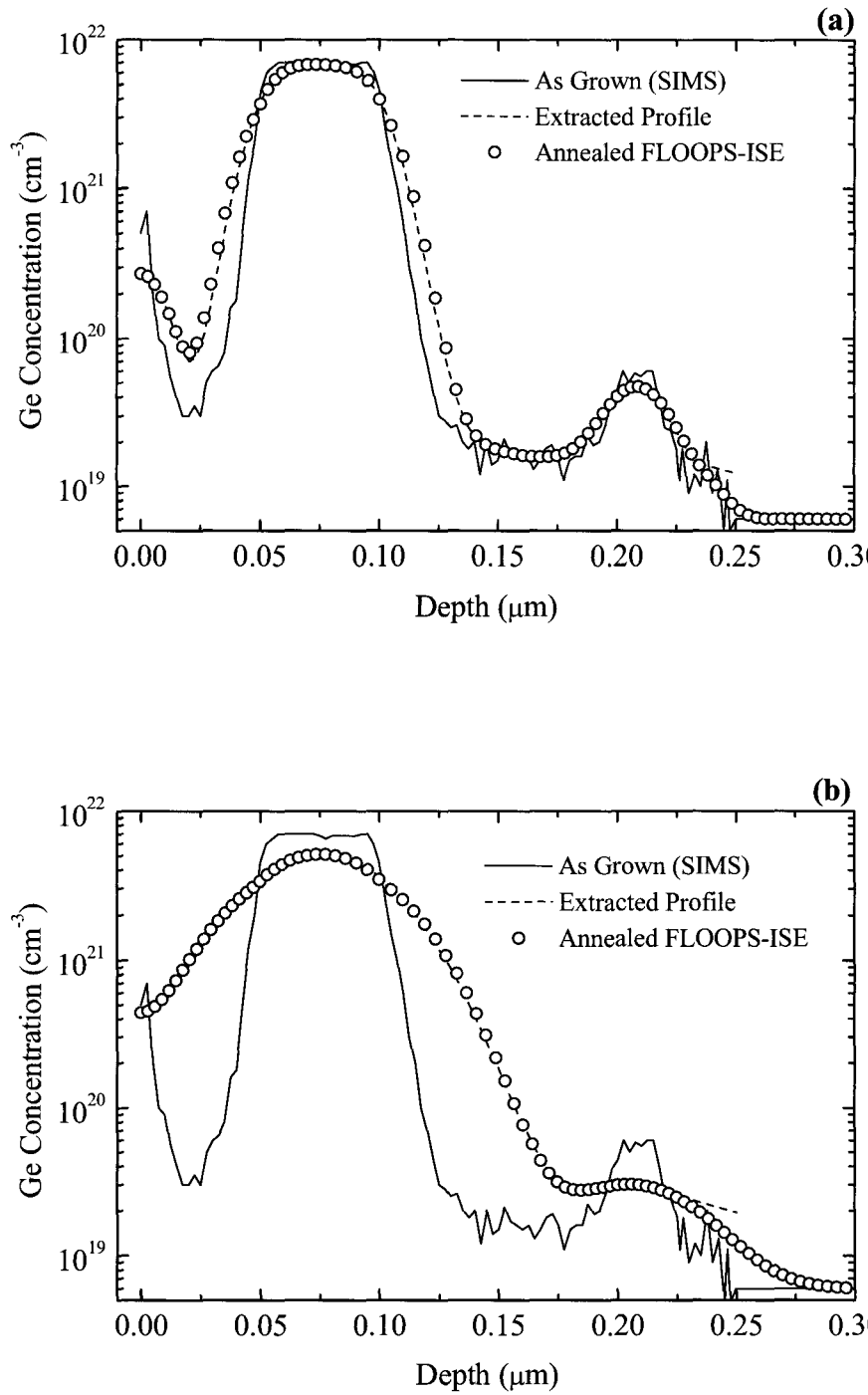

Figure 5.1: Comparison between extracted experimental Ge profile and simulated Ge profile for samples annealed in inert ambient at 900°C for (a) 330 min and (b) 2206 min.

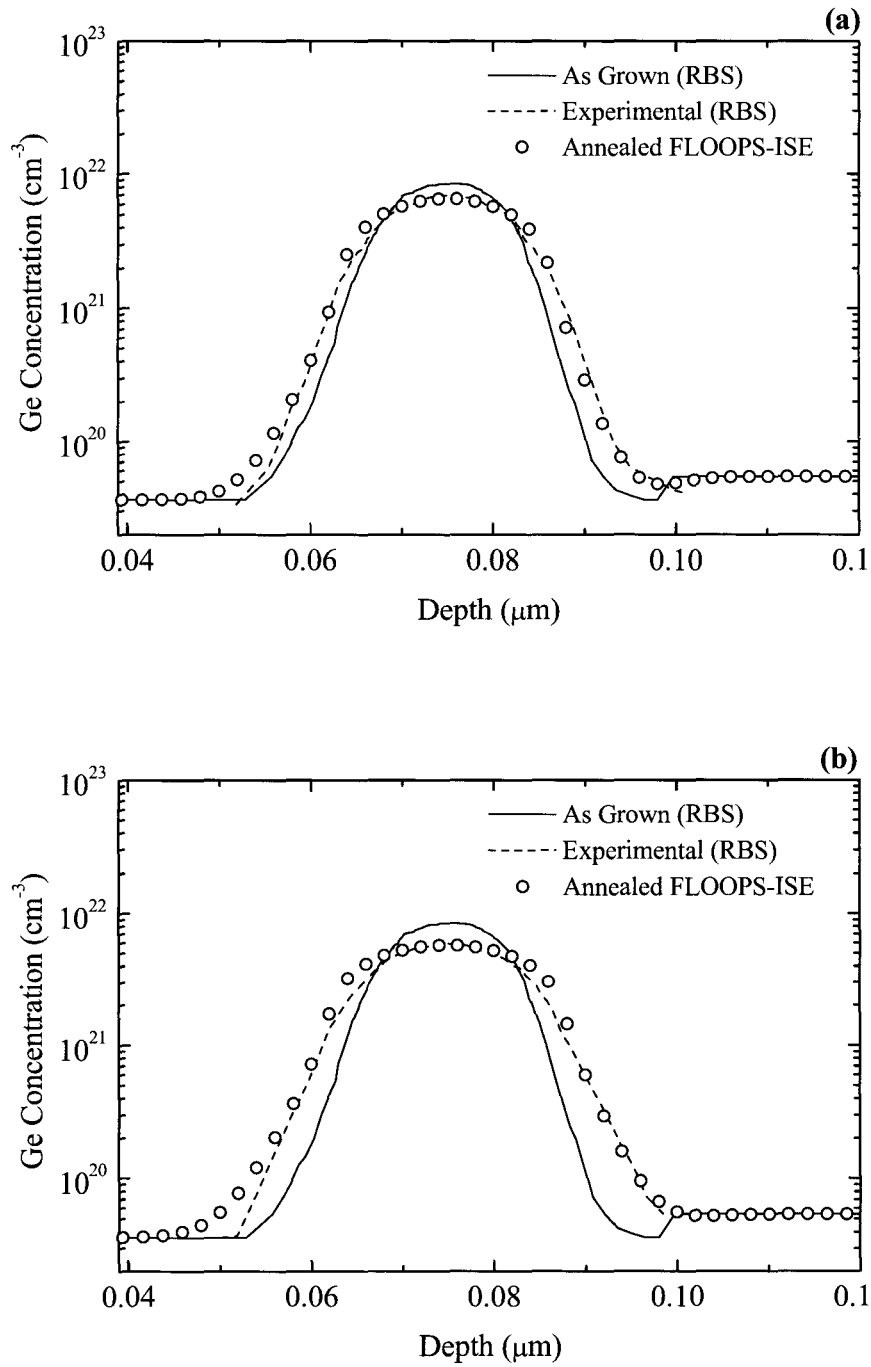

Figure 5.2: Comparison between experimental Ge profile and simulated Ge profile for samples annealed in inert ambient at 970°C for (a) 30 min and (b) 60 min.

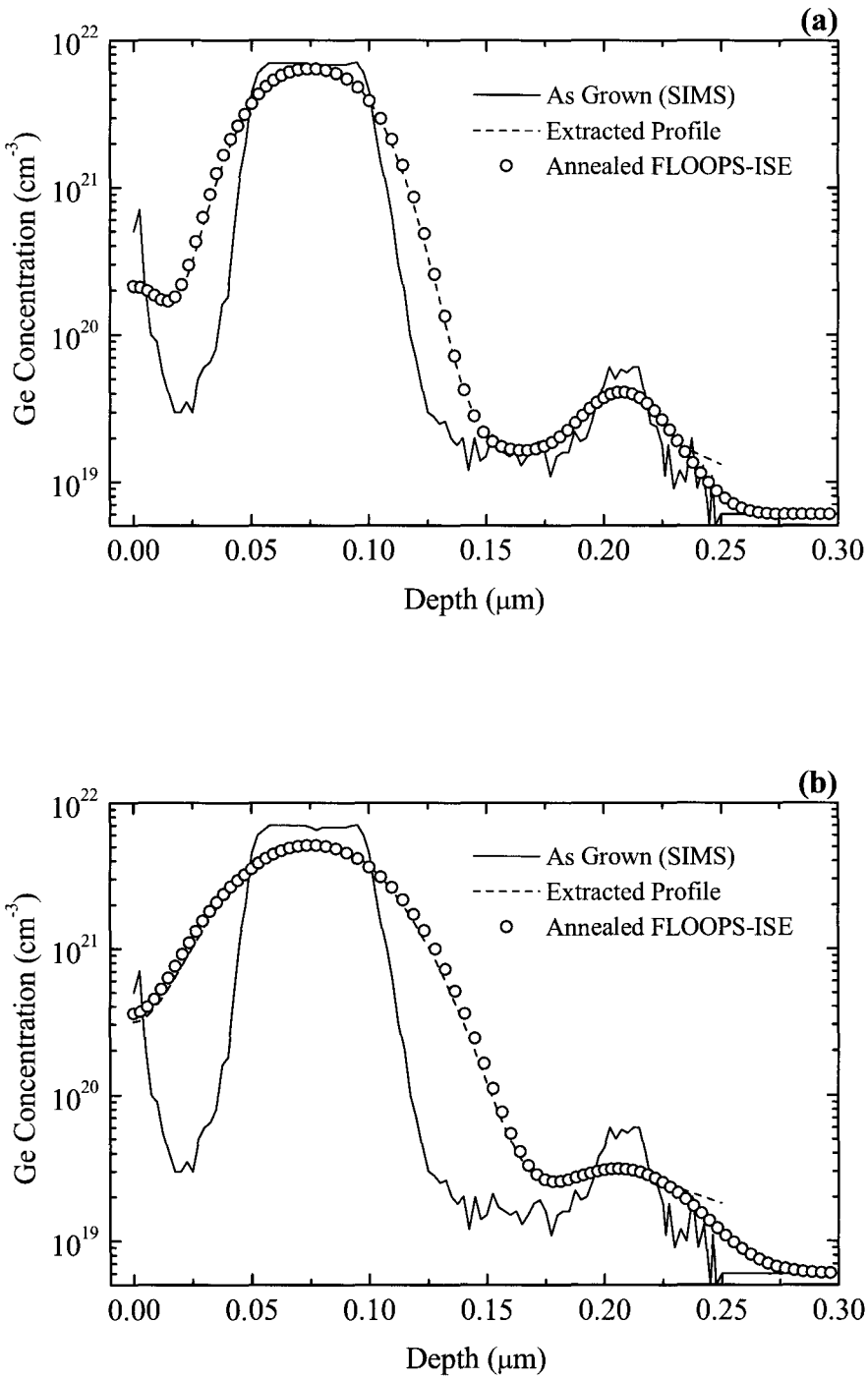

Figure 5.3: Comparison between extracted experimental Ge profile and simulated Ge profile for samples annealed in inert ambient at 1000°C for (a) 43 min and (b) 125 min.

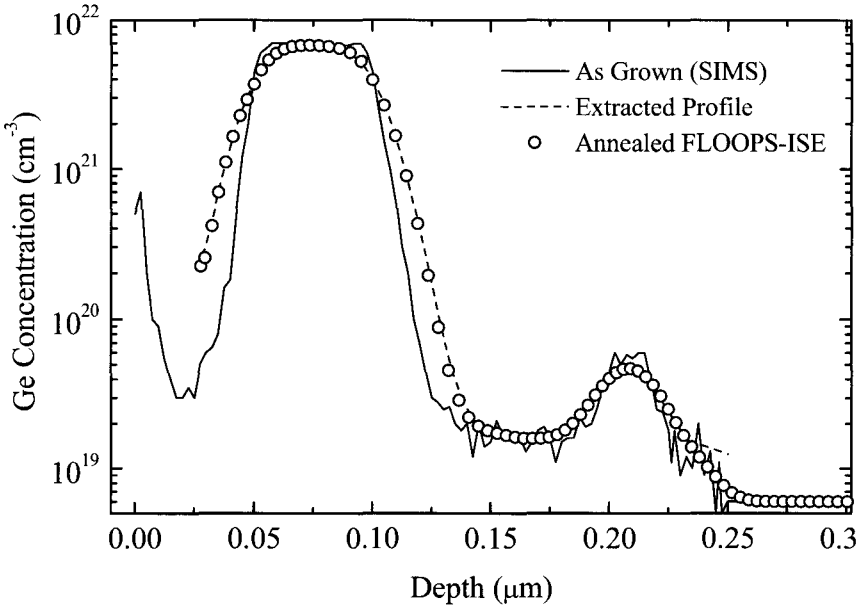

Figure 5.4: Comparison between extracted experimental Ge profile and simulated Ge profile for samples annealed in oxidizing ambient at 900°C for 330 min.

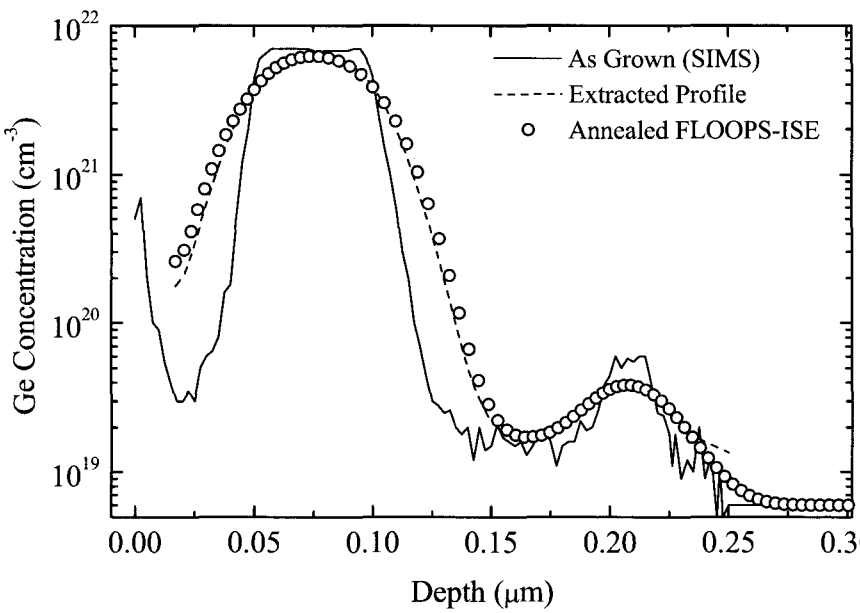

Figure 5.5: Comparison between extracted experimental Ge profile and simulated Ge profile for samples annealed in oxidizing ambient at 1000°C for 43 min.

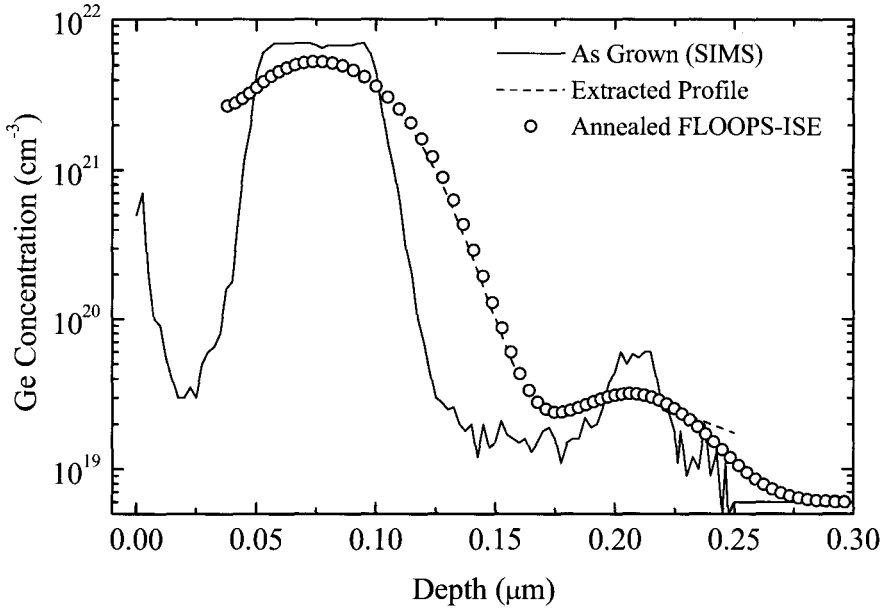

Figure 5.6: Comparison between extracted experimental Ge profile and simulated Ge profile for samples annealed in oxidizing ambient at 1000°C for 125 min.

Figure 5.7 and Figure 5.8 respectively show a comparison between the best fit values for D_{Si}^{*} and D_{Ge}^{*} compared with the literature. The values of D_{Si}^{*} are compared with the values reported by Laitinen *et al.* [33] and Borg and Dienes [58]. The values of D_{Ge}^{*} are compared with the values reported by Zangenberg *et al.* [34] and Sharma [59]. The close match observed confirms that the vacancy exchange mechanism is sufficient to explain interdiffusion phenomena in Si/SiGe heterostructures.

As mentioned in Section 5.1, the initial profile of intrinsic equilibrium vacancy concentration (C_V^{*}) in the structure was varied during the simulation as a function of Ge fraction. In Si, C_V^{*} was kept equal to its default value in FLOOPS-ISE. We

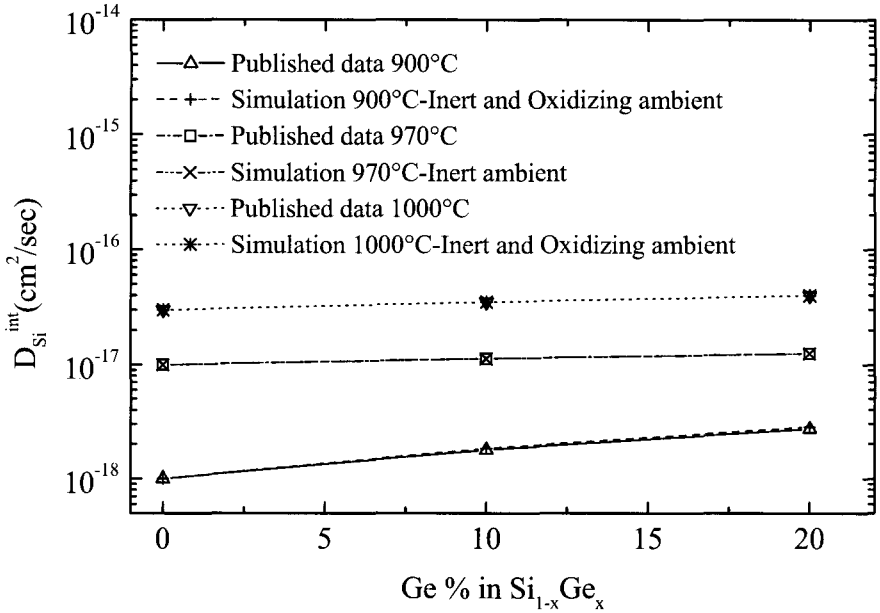

Figure 5.7: D_{Si}^{*} used in the simulations compared to previously published results [33], [58].

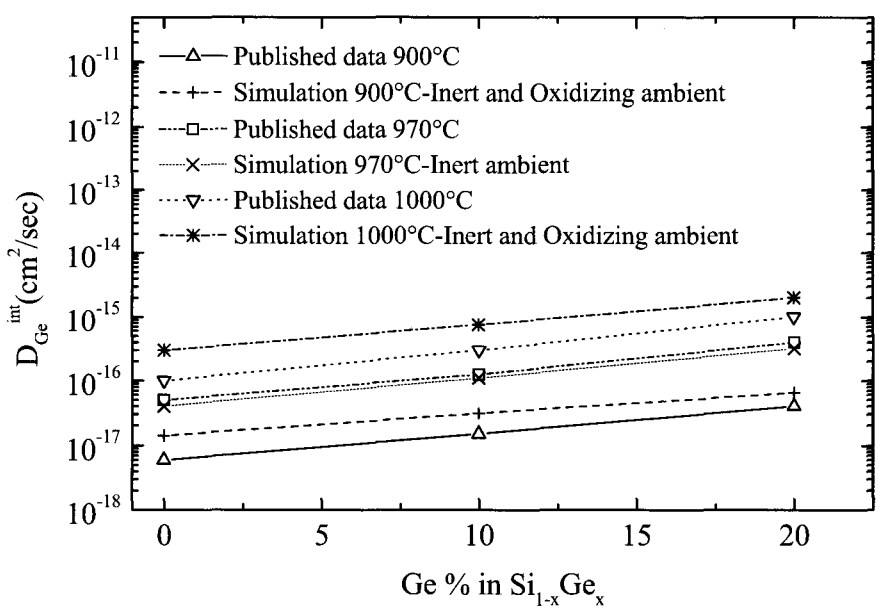

Figure 5.8: D_{Ge}^{*} used in the simulations compared to previously published results [34], [59].

surveyed the literature on values for C_V^* in SiGe as a function of Ge fraction but were unable to discover reliable quantitative data in the temperature range of the study. However, there is general agreement that both the presence of Ge and compressive strain increase the equilibrium concentrations of vacancies [56]-[57]. For the structures studied here, this leads to the expectation that in $Si_{1-x}Ge_x$ the value of C_V^* is higher than that in Si. Thus during the simulations the values of C_V^* in $Si_{1-x}Ge_x$ in the initial profile were set higher than the corresponding values in Si. Initially the values of C_V^* in $Si_{1-x}Ge_x$ were increased compared to the values in Si and the simulated Ge interdiffusion profiles were observed. The initial increase in C_V^* values did not show any significant influence on the simulated Ge interdiffusion profiles. After the values of C_V^* were increased above certain values, the simulated Ge interdiffusion profiles were non-Gaussian in nature. As the experimental profiles were Gaussian in nature, the maximum values of C_V^* up to which the simulated Ge interdiffusion profiles remained Gaussian were taken as upper bounds on C_V^* in SiGe. Figure 5.9 shows these upper bound values used in simulation in SiGe compared to the corresponding default values in FLOOPS-ISE for pure Si. As seen from the figure the values used for C_V^* in SiGe show Arrhenius behavior as in pure Si and in all the cases the values of C_V^* in SiGe are approximately 1.3 times higher than the corresponding values in pure Si.

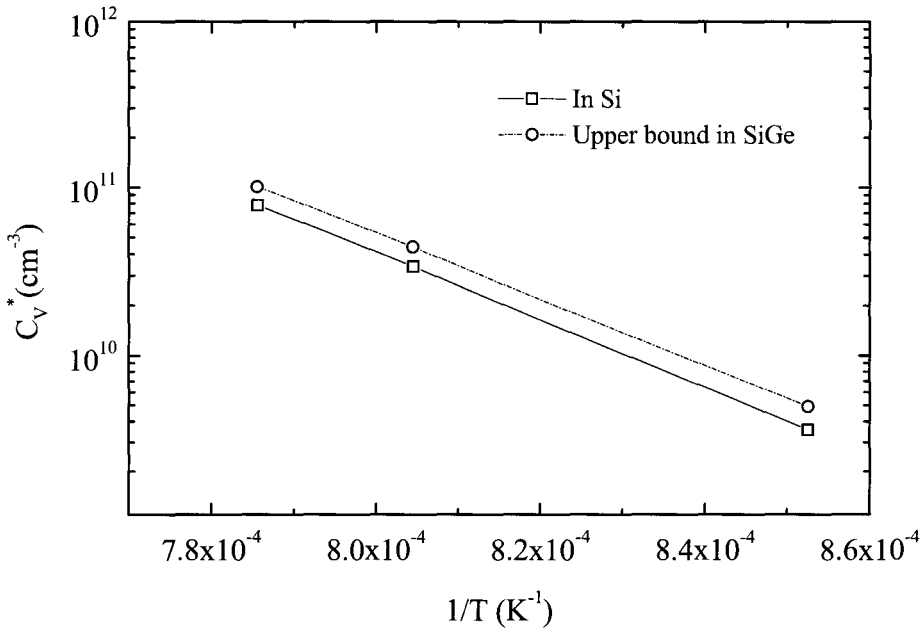

Figure 5.9: Comparison of initial profile values of C_V^* used in SiGe compared to the corresponding values in pure Si.

5.3 Interdiffusion at Temperatures Above 1050°C

Figure 5.10 and Figure 5.11 show the values of D_{Si}^* and D_{Ge}^* that would be required at 1100 and 1200°C to obtain good fits to the inert and oxidizing anneals at those temperatures using only the vacancy exchange mechanism. In all cases, the values obtained are about an order of magnitude higher than published values. (At 1200°C the values required for the oxidizing anneal are slightly lower than those for the inert anneal, but the difference is well within the error margin). This would seem to indicate that the vacancy exchange model by itself is not sufficient to model these results. This is also consistent with the knowledge that in pure Si interstitials play a dominant role at

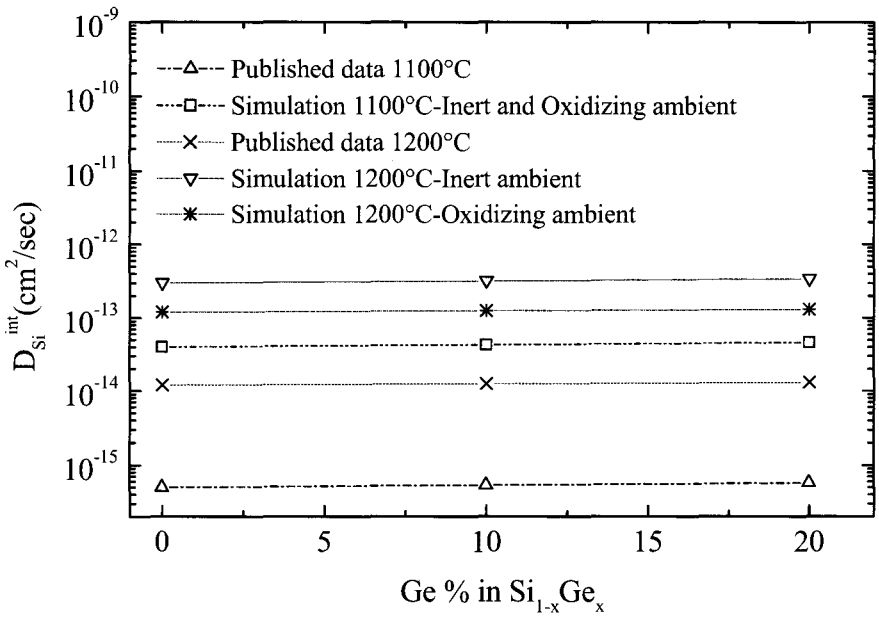

Figure 5.10: D_{Si}^{*} used in the simulations compared to previously published results [33], [58].

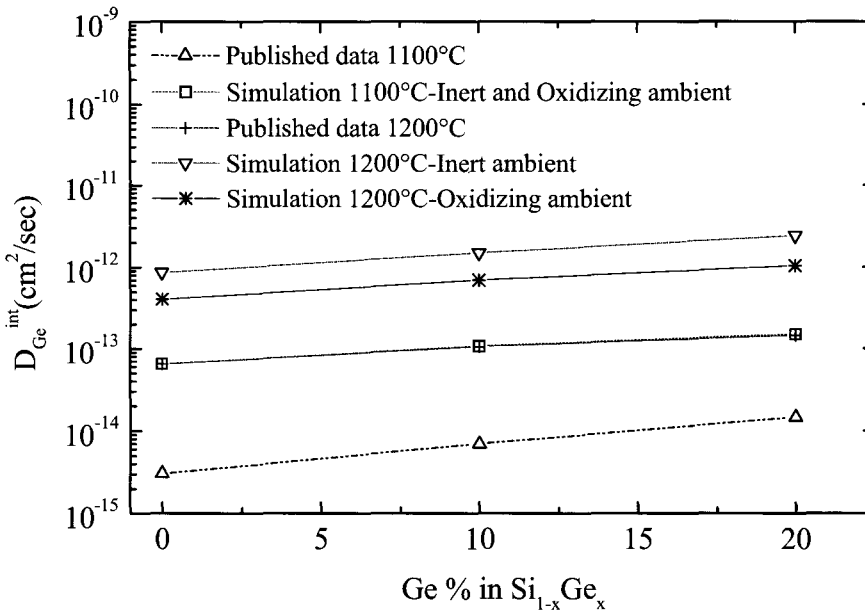

Figure 5.11: D_{Ge}^{*} used in the simulations compared to previously published results [34], [59].

temperatures above 1050°C and that with 15% Ge one would expect behavior closer to that of pure Si than that of pure Ge.

As the vacancy exchange mechanism alone is not sufficient to model the interdiffusion mechanism in the structure at 1100 and 1200°C, to model the interdiffusion mechanism at these temperatures both in inert and oxidizing ambients, the effects of interstitials in the interdiffusion mechanism are considered next along with the vacancy exchange mechanism. The detailed mathematical formulation of the model has been given in Chapter 4. The fitting parameters used while applying the model were the intrinsic self-diffusivities of Ge and Si (D_{Ge}^{*} and D_{Si}^{*}), the interstitial Si diffusivity (D_{Si_I}), the interstitial Ge diffusivity (D_{Ge_I}) and the equilibrium concentrations of Si and Ge interstitials as well as vacancies. The variations of D_{Ge}^{*}, D_{Si}^{*} and C_V^{*} as a function of Ge fraction were discussed in the previous section. The variations of the equilibrium concentrations of Si and Ge interstitials with Ge fraction are discussed in detail below (Section 5.3.1). Fitting parameters were set in such a way that keeping these fixed for a given temperature and anneal conditions, good matches between the simulated Ge interdiffusion profiles and the extracted experimental Ge interdiffusion profiles were observed as the anneal times were varied.

At these temperatures, Griglione *et al.* [44] also provided data on nitriding anneals. To prove successful, the model must also extend to these data. This creates an additional problem that we did not have to address in the low temperature case because no data from nitridation experiments were available there. For the temperature range above 1050°C, we have to model interdiffusion in inert, oxidizing, and nitriding ambients. In the nitriding ambient case, it is known that nitridation of Si causes vacancy injection, but no

quantitative model is available in the literature, and none is provided in FLOOPS-ISE. Therefore, we had to quantify vacancy injection during nitridation of pure Si based on published data, and this is discussed in detail below (Section 5.3.2).

5.3.1 Equilibrium Concentration of Si and Ge Interstitials

Both the Ge fraction and the strain in the layers are expected to affect the equilibrium concentration of Si interstitials in the structure. The effect of pressure on this parameter was neglected and this parameter was varied in the simulation as the Si/Ge interdiffusion in the structure occurred using the following relation [8],

$$C^*_{Si_I} = C^*_{Si_I}(Si)e^{-\Delta V_{GeI}/kT} \tag{5.2}$$

$$\Delta V_{GeI} = \Delta V_{olGeI} . a_{SiGe} . \frac{C_{Ge}}{5x10^{22}} \tag{5.3}$$

where, $C^*_{Si_I}(Si)$ is the equilibrium concentration of Si interstitial in pure Si, ΔV_{GeI} is the total activation volume change of equilibrium interstitial due to the presence of Ge. ΔV_{GeI} can be calculated from the Ge fraction in the structure (C_{Ge}), lattice mismatch parameter a_{SiGe}, and the activation volume change ΔV_{olGeI} as shown on equation (5.3). As the lattice constant in SiGe varies as the Ge fraction changes, considering Vegard's rule given in equation (1.1), the lattice constant in the structure was calculated taking into account the Ge interdiffusion phenomena. Based on the calculated lattice constant the lattice misfit parameter a_{SiGe} was calculated. The value of ΔV_{olGeI} was set to 11.8 eV which is the default value in FLOOPS-ISE.

The variation of equilibrium interstitial Ge concentration with Ge is expected to follow the same trend as above. However, the relative magnitude would be expected to be

lower than that of the Si interstitials because of the size considerations. In our simulations, we set the equilibrium concentration of Ge interstitials to be proportional to that of the Si interstitials and used the proportionality constant as a fitting parameter.

5.3.2 Vacancy Injection During Nitridation of Si

As vacancy injection during nitridation of Si is not modeled in FLOOPS-ISE, the first step to model the nitriding ambient Ge interdiffusivity in $Si/Si_{1-x}Ge_x/Si$ SQW structure is to model the vacancy injection itself. To do this two previously reported results [60]-[61] dealing with nitridation of Si were taken as reference. In both studies the diffusion of antimony (Sb) was compared in inert vs. nitriding ambient. As Sb is believed to be a vacancy diffuser with diffusivity directly proportional to the local vacancy concentration, observation of Sb diffusivity gives a measure of the vacancy injection during nitridation of Si. Mogi *et al.* [60] studied Sb diffusion at 810, 860, and 910°C for 15-180 min annealing and reported average intrinsic Sb diffusivity values $\langle D_{Sb}^{INT} \rangle$ which were normalized to the inert intrinsic Sb diffusivities and reported as a function of sample depth. These values in fact represent time average vacancy concentrations normalized to the inert equilibrium vacancy concentration, $\langle C_V \rangle / C_V^*$. The reported values by Mogi *et al.* [60] are shown in Figure 5.12 (a)-(c). A similar experiment was published earlier by Fahey *et al.* [61] where Sb diffusion was observed 1100°C for a long range of annealing times. They also reported values of average intrinsic Sb diffusivity values $\langle D_{Sb}^{INT} \rangle$ normalized to inert intrinsic Sb diffusivities. We considered these values as $\langle C_V \rangle / C_V^*$ and are shown in Figure 5.12 (d).

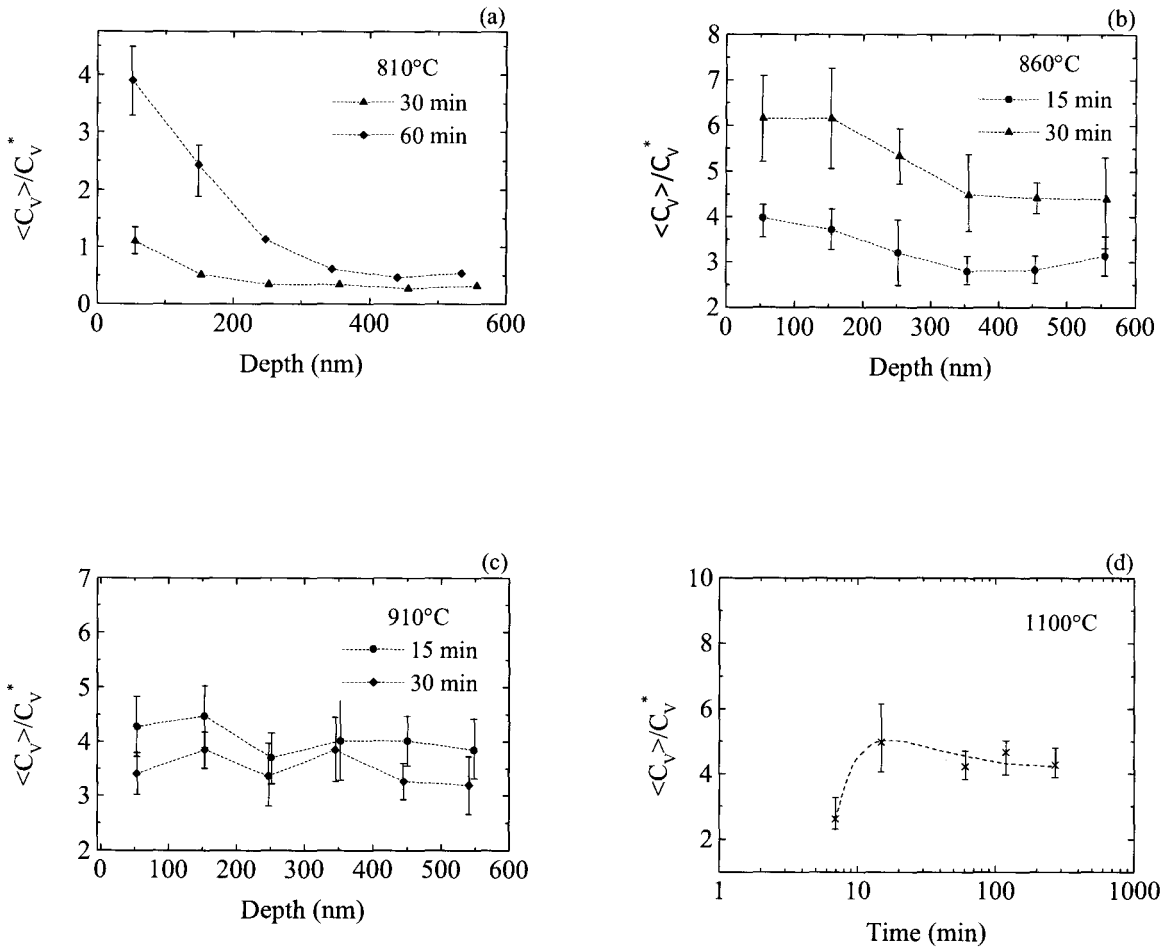

Figure 5.12: Mogi *et al.* [60] reported $\langle C_V \rangle / C_V^*$ at (a) 810°C, (b) 860°C, (c) 910°C and (d) Fahey *et al.* [61] reported $\langle C_V \rangle / C_V^*$ at 1100°C.

Based on these two studies reported, attempts were made to model the injection of vacancies during nitridation of Si. To model the vacancy injection, we impose a flux equation at the nitride/Si interface of the form,

$$Vac\_Inj - K \times (Vac\_Silicon - EqVac\_Silicon) \tag{5.4}$$

where, *Vac_Inj* is the vacancy injection term and K represents a surface recombination term.

At first the flux equation mentioned above was applied for the results reported by Mogi *et al.* [60]. *Vac_Inj* and *K* were adjusted so that for each of the temperatures 810, 860 and 910°C, keeping these parameters fixed, the value $\langle C_V \rangle / C_V^*$ becomes equal to the values reported by Mogi *et al.* [60] at two different depths, 150 and 400 nm, for two different anneal times.

For 1100°C, the results reported by Fahey *et al.* [61] were considered. For this case *Vac_Inj* and *K* were adjusted so that at 150 nm depth, for two different anneal times, the values of $\langle C_V \rangle / C_V^*$ were equal to the values reported by Fahey *et al.* [61].

Figure 5.13 and Figure 5.14 show respectively the variation of *Vac_Inj* and *K* as a function of temperature fixed by the above procedures to model the vacancy injection during nitridation of Si. Both *Vac_Inj* and *K* show Arrhenius behavior. The best fit lines are given by:

$$Vac\_Inj = 2.45 \times 10^{41} \exp(-8.65eV / kT) \tag{5.5}$$

$$K = 1.39 \times 10^{20} \exp(-6.29eV / kT) \tag{5.6}$$

These values of *Vac_Inj* and *K* were used in the flux equation represented by equation (5.4) to model vacancy injection during the nitriding ambient simulations.

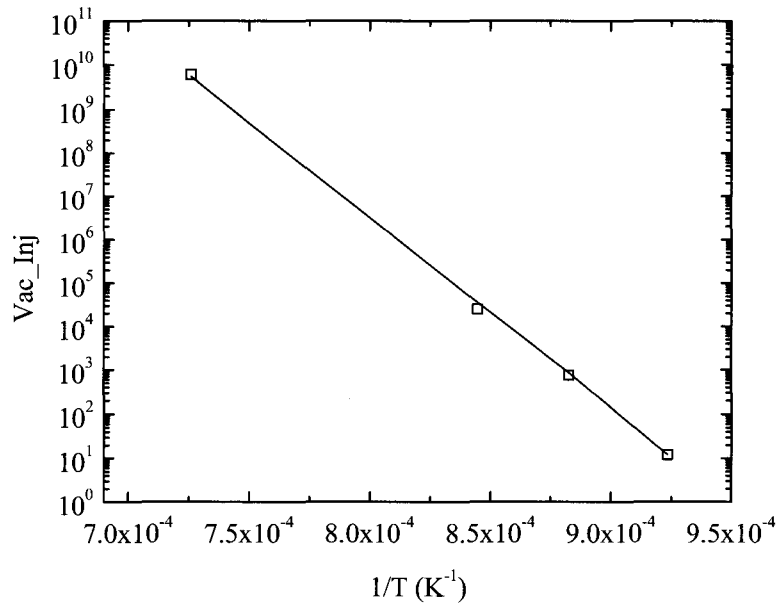

Figure 5.13: Variation of *Vac_Inj* as a function of temperature.

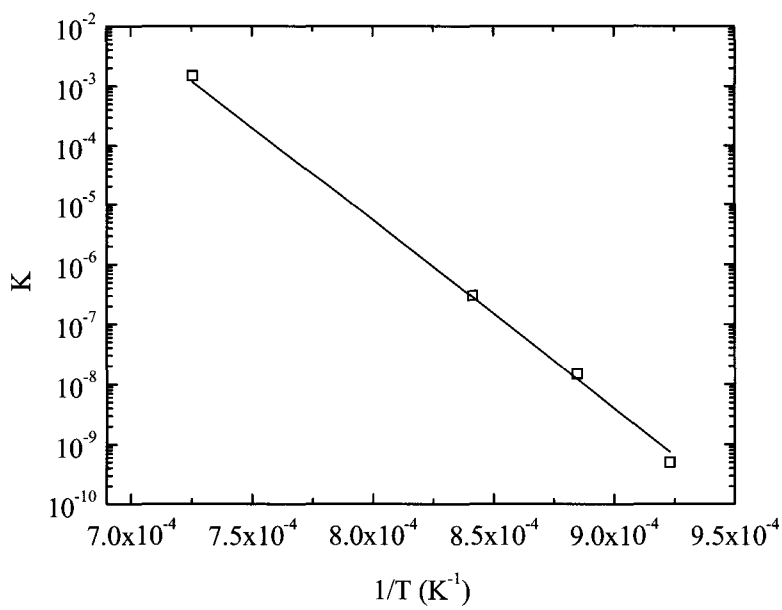

Figure 5.14: Variation of *K* as a function of temperature.

5.3.3 Simulation Results

Figure 5.15, Figure 5.16 and Figure 5.17 respectively show typical fits between the simulated Ge interdiffusion profile and extracted experimental Ge interdiffusion profile for samples annealed in inert, oxidizing and nitriding ambients for 2 min anneal at 1100°C. Figure 5.18 and Figure 5.19 respectively show typical fits between the simulated Ge interdiffusion profile and extracted experimental Ge interdiffusion profile for samples annealed in inert and oxidizing ambient for 1.5 min anneal at 1200°C. Figure 5.20 shows typical fits between the simulated and extracted experimental Ge interdiffusion profile in nitriding ambient for 1 min anneal at 1200°C.

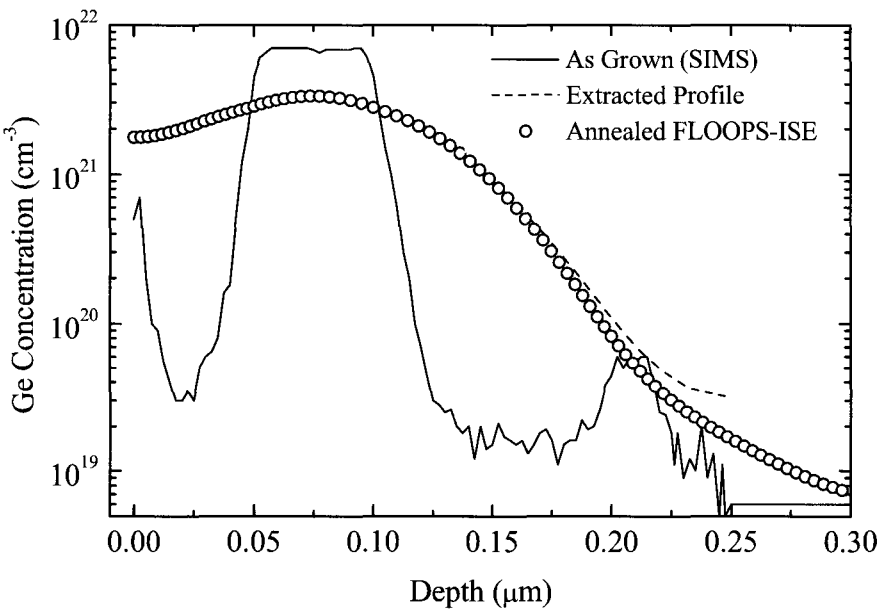

Figure 5.15: Comparison between extracted experimental Ge profile and simulated Ge profile for samples annealed in inert ambient at 1100°C for 2 min.

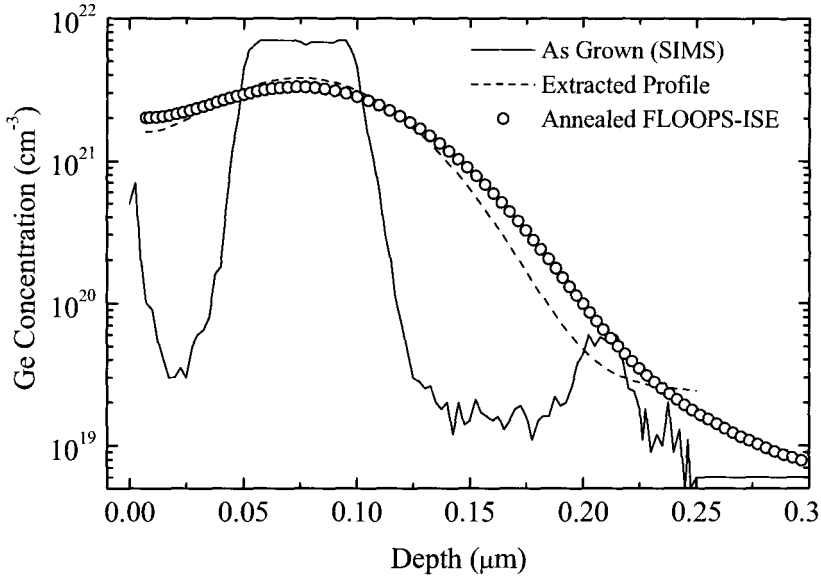

Figure 5.16: Comparison between extracted experimental Ge profile and simulated Ge profile for samples annealed in oxidizing ambient at 1100°C for 2 min.

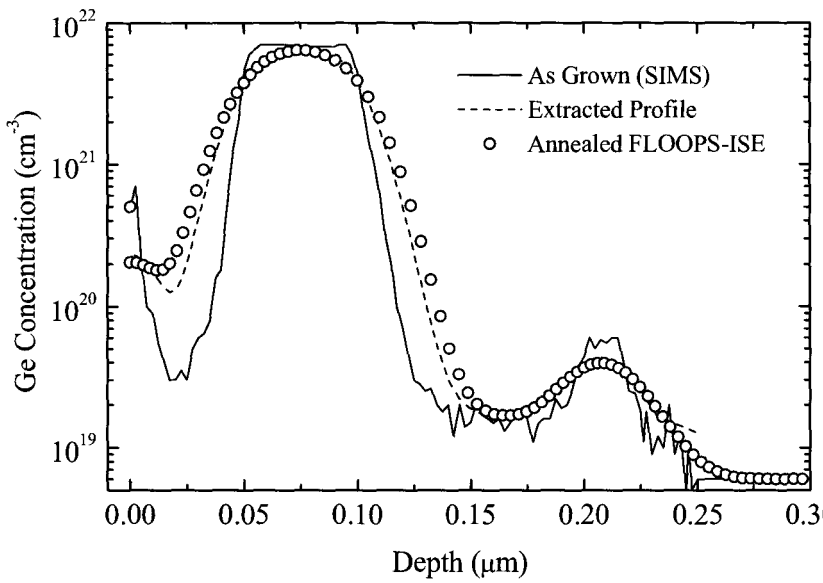

Figure 5.17: Comparison between extracted experimental Ge profile and simulated Ge profile for samples annealed in nitriding ambient at 1100°C for 2 min.

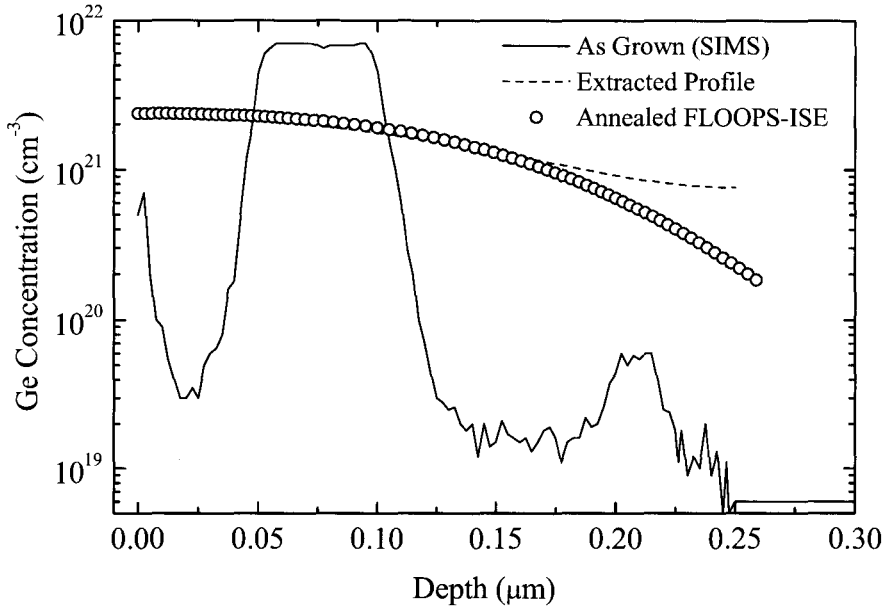

Figure 5.18: Comparison between extracted experimental Ge profile and simulated Ge profile for samples annealed in inert ambient at 1200°C for 1.5 min.

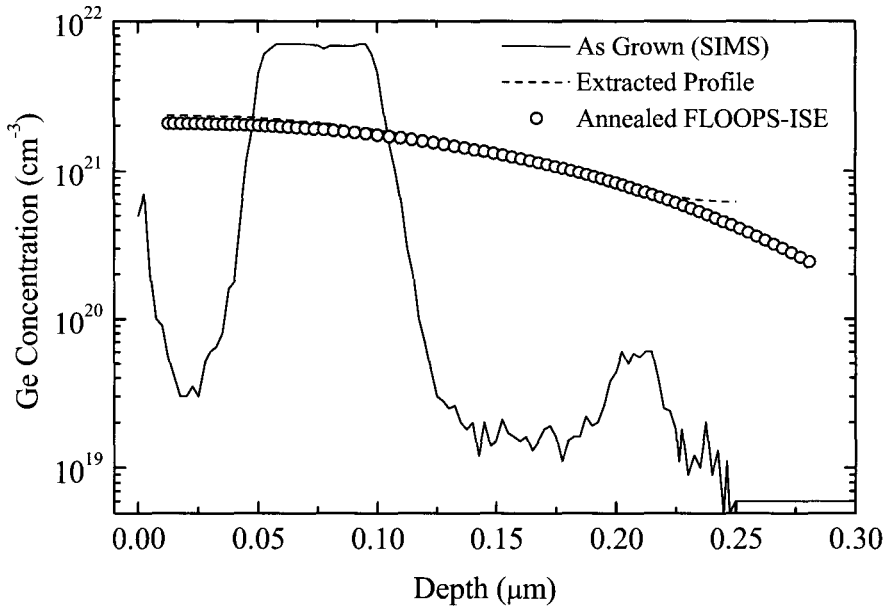

Figure 5.19: Comparison between extracted experimental Ge profile and simulated Ge profile for samples annealed in oxidizing ambient at 1200°C for 1.5 min.

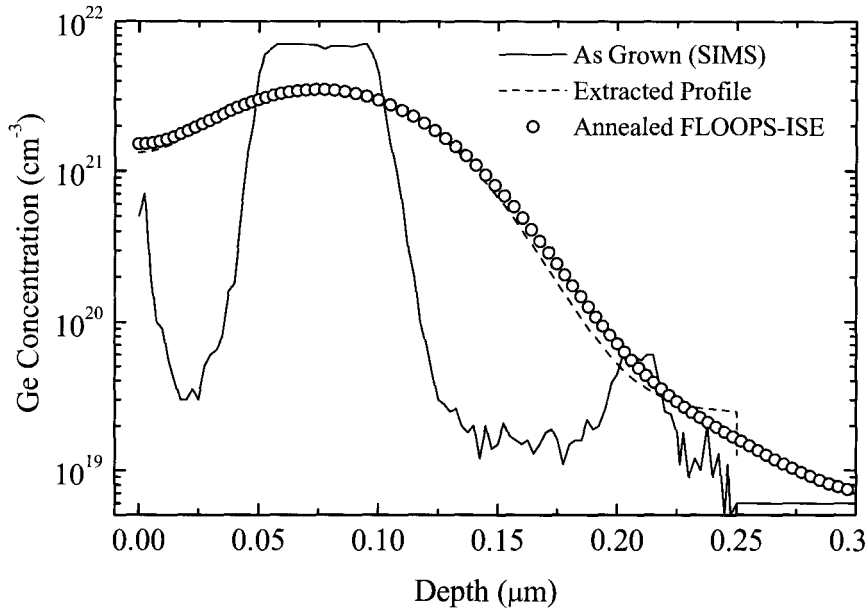

Figure 5.20: Comparison between extracted experimental Ge profile and simulated Ge profile for samples annealed in nitriding ambient at 1200°C for 1 min.

5.3.4 Simulation Parameters

Given the above analysis, we know D^*_{Ge} and D^*_{Si}, we know the diffusivities of the Si interstitials and the equilibrium concentrations of the vacancy and the interstitial Si in pure Si, and we have a reasonable idea of the variation of these as a function of Ge fraction. We also know the parameters for vacancy injection during nitridation and can use the default parameters from FLOOPS-ISE for interstitial injection during oxidation. The only remaining unknowns are the diffusivity and equilibrium concentration of the Ge interstitial. During the simulations we found that unless these parameters were set orders of magnitude higher than the corresponding values for the Si interstitials, the simulation was insensitive to variations of these numbers. This indicates that the Si interstitial, not

the Ge, is the rate limiting step. In the simulations, we arbitrarily set the equilibrium concentration of the Ge interstitial to be two orders of magnitude below that of the Si interstitial, and the diffusivity of the Ge interstitial to be equal to that of the Si interstitial.

With these remarks, the model has no further free parameters. For *both* the oxidizing and nitriding cases, this model the parameters set as above accurately fits the experimental results. Typical fits in oxidizing and nitriding ambients are shown in Figures 5.16-5.17 and Figures 5.19-5.20 for 1100 and 1200°C. The values of D_{Ge}^{*} and D_{Si}^{*} are taken directly from the literature [33], [34], [58], [59]. The values of D_{Si_I} and $C_{Si_I}^{*}(Si)$ are the same as the default FLOOPS-ISE values, and $C_{Si_I}^{*}(Si)$ is considered to vary with Ge per equations (5.2)-(5.3).

Unfortunately, using these parameters the diffusion for the inert case is considerably underestimated. In order to match the experimental results for the inert case, it is necessary to increase either vacancy components of the diffusion (by increasing D_{Ge}^{*} and D_{Si}^{*}) or the interstitial components (by increasing D_{Si_I} and/or $C_{Si_I}^{*}(Si)$). The required total increase is one order of magnitude (~10 ×) over the present set of parameters. By following this approach the typical fits we get are shown in Figure 5.15 and Figure 5.18 for 1100 and 1200°C. In Section 5.4, we discuss this problem in more details.

5.3.5 Understanding the Contribution of the Different Mechanisms

Now to get an idea of the contribution of only the vacancies in the interdiffusion process, the published values of D_{Ge}^{*} and D_{Si}^{*} for 1100 and 1200°C are used in the simulations considering only the vacancy exchange mechanism. By taking this approach

it is possible to observe the contribution of vacancies in the overall interdiffusion mechanism. It is seen that the interdiffusion of Ge with only the vacancy exchange mechanism using these values of D_{Ge}^{*} and D_{Si}^{*} is small compared to the final diffusion of Ge both at 1100 and 1200°C. This suggests that at 1100 and 1200°C interstitials play a major role in the interdiffusion phenomena. Figure 5.21 shows the simulated interdiffusion profile of Ge considering only the vacancy exchange mechanism and using the above values of D_{Ge}^{*} and D_{Si}^{*} for samples annealed in oxidizing ambient for 3 min at 1100°C. This indicates that at these temperatures, the dominant diffusion mechanism is interstitial diffusion and for nitriding ambient a vacancy injection slows down the diffusion through recombination with interstitials.

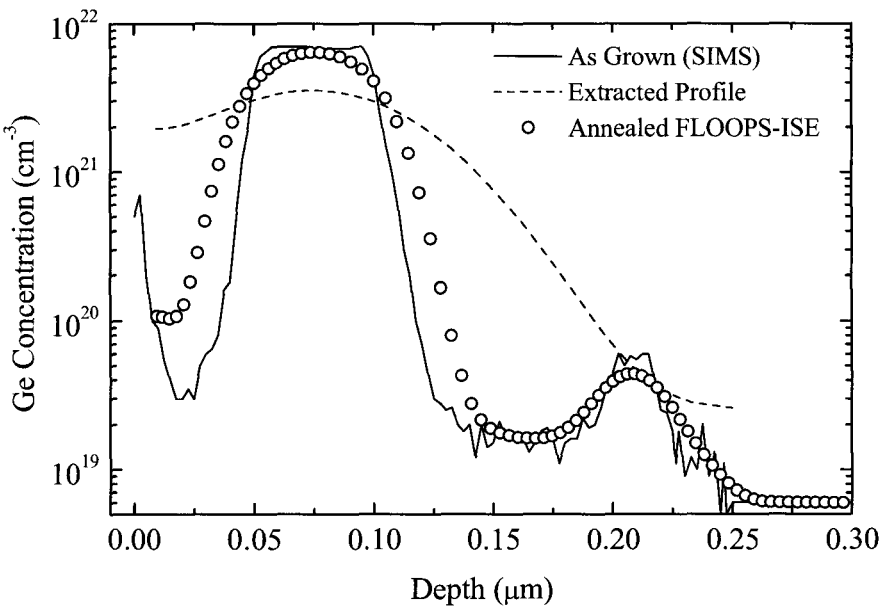

Figure 5.21: Comparison of simulated Ge interdiffusion profile with extracted experimental Ge interdiffusion profiles for 3 min anneal in oxidizing ambient at 1100°C using intrinsic self-diffusivities of Si and Ge reported at literature [33], [34], [58], [59].

5.4 Discussion of the Inert Anneals at High Temperatures

As mentioned in the foregoing section, while the results under oxidizing and nitriding ambient provide a coherent picture of the interdiffusion process, the inert anneal results cannot be predicted using the parameters set consistent with our knowledge of SiGe material properties and consistent with other experimental results. It should be noted that a match could be obtained by slightly increasing each of the four effective parameters in the model (D^*_{Ge}, D^*_{Si}, D_{Si_I}, and $C^*_{Si_I}(Si)$). Since the total enhancement observed is about an order of magnitude, the enhancement to each of the four parameters would be small. The argument for doing this is that the variation in each parameter would be within the accuracy of estimating that parameter. However, such an approach ignores the low likelihood of systematic and cumulative random errors in the four parameters separately.

A second possibility is of some anomaly in the processing of the high temperature samples under an inert ambient. The high temperature samples from the Griglione *et al.* [43]-[44] studies were annealed in an RTA chamber, whereas the low temperature experiments were furnace anneals. It is possible that some oxygen contamination of the RTA chamber was responsible for the enhanced diffusion.

Yet a third possibility is that the multiple difficulties indicated by Griglione *et al.* in their study compounded to produce the observed effect. The authors [43]-[44] note that the samples annealed at high temperatures partially relaxed by forming dislocations. Additionally, their estimate of the interstitial injection during oxidation was lower than expected. This would indicate that these samples should have a higher inert diffusivity but a lower enhancement to the diffusivity under oxidation. Such an explanation would fit

our model for the inert and oxidizing case. However, it would predict enhanced diffusion in the nitriding case.

The available data is not sufficient to conclusively resolve this issue. We discuss ideas for further work, both modeling and experimental, in Chapter 6.

Chapter 6

CONCLUSIONS

The aim of this thesis was to model the Si-Ge interdiffusion mechanism in a $Si/Si_{1-x}Ge_x/Si$ single quantum well structure. The success of the model would be indicated by its ability to model the interdiffusion in samples annealed over a wide range of temperatures for varying anneal times in inert, oxidizing and nitriding ambients. In Chapter 3, a survey of existing interdiffusion studies was presented. In these studies various experimental techniques were utilized to measure the extent of interdiffusion. The information was usually presented in the form of an overall interdiffusivity. However, there have been no attempts in the literature to provide a qualitative physically based model of the interdiffusion process.

Chapter 4 described the mathematical models applied in this study. Based on these models simulation results were reported in Chapter 5. The model parameters were consistent with previously reported data. The following sections summarize the contributions made in this work and suggestions for future works.

6.1 Contributions

This thesis provides the first implementation of a quantitative model of interdiffusion that takes into account the contributions of both vacancies and interstitials in a semiconductor binary alloy. The model was applied to Si-Ge interdiffusion and yielded considerable insight into the process.

The mathematical model for the vacancy exchange mechanism for interdiffusion was demonstrated to adequately explain published Si-Ge interdiffusion results at low temperatures (below 1050°C) both in inert and oxidizing ambients using well established published values for the self-diffusion coefficients of Si and Ge. Additionally, an upper bound was established for the equilibrium vacancy concentration in a SiGe alloy with 15 and 17% Ge content.

For high anneal temperatures (above 1050°C), the contributions of interstitials along with the vacancy exchange mechanism were shown to have considerable impact on the diffusion process. It was demonstrated that a model taking into account the contribution of both vacancies and interstitials fully accounts for the interdiffusion behavior under conditions of interstitial injection and vacancy injection. Once again, the well established values of Si and Ge self-diffusivities were used. Additionally, the well established parameters describing the behavior of the Si interstitial in pure Si were used. The remaining free parameters of the model (the properties of Ge interstitial) were found to have little impact on the diffusion behavior, indicating that the diffusion of Si interstitial is the rate limiting step for the diffusion at these temperatures. The available experimental data on inert diffusion could not be interpreted consistently with the rest of the data and this remains a topic for further investigation.

The foregoing results are important to the debate on the diffusion mechanism in SiGe. We have demonstrated (a) that for 15 and 17% Ge the behavior is more akin to the case of pure Si where the dominant point defect is different in temperature regimes; and (b) that even when a single activation energy is extracted from the effective diffusivities (as was the case with Griglione *et al.* data) two different mechanisms may be responsible for the diffusion in different temperature regimes. Our model provides a quantitative method of determining the contribution of each diffusion mechanism to the overall diffusion behavior.

Finally, this study provides the first quantitative description of vacancy injection during nitridation of Si over a broad temperature range. Combining previous reported results with our own modeling of Si-Ge interdiffusion, we have provided quantitative expressions for the generation and surface recombination components of the vacancy injection flux from the nitriding interface.

6.2 Suggestions for Future Works

In this study we have proposed mathematical models for interdiffusion of Si/Ge in $Si/Si_{1-x}Ge_x/Si$ single quantum well structure. There are several fitting parameters including the intrinsic self-diffusivity of Si and Ge, the diffusivity of interstitial Si and Ge, and the equilibrium concentrations of Si and Ge interstitials as well as vacancies. In the course of the study it has become clear that experimentally reported values of diffusivity of interstitial Ge and equilibrium interstitial concentration of Ge are not available. In this study, these appeared to have little impact on the diffusion behavior. Nonetheless, it is of fundamental interest to design experiments that would yield values for the diffusivity of interstitial Ge and equilibrium interstitial concentration of Ge. Another parameter that

requires further experimental verification is variation of the inert equilibrium vacancy concentration as a function of Ge fraction.

For temperatures at 1100 and 1200°C, the mathematical model considering the role of interstitials along with vacancy exchange mechanism was not adequate to interpret interdiffusion results in samples annealed in inert ambient. Thus it is necessary to study the inert ambient interdiffusion phenomenon more carefully to understand the actual interdiffusion mechanism at inert ambient for high anneal temperatures.

In general, there appears to be a lack of experimental studies of Si-Ge interdiffusion. Experimental work is needed to provide data for different Ge fractions with stable strained layers that do not form extended defects during the course of annealing.

In this study the mathematical models were applied only to single quantum well structure. The models can be applied to other types of heterostructures (e.g., superlattices) to check the validity of the model. Also it will be interesting to see whether the interdiffusion mechanism depends on the Ge fraction present in the structures. Again, experimental data will be required beyond what is currently available in the literature.

The modeling performed in this study was done in intrinsic samples. However all the practical devices are extrinsically doped. Thus it is important to study interdiffusion mechanism under extrinsic doping condition. The presence of dopants and the resulting shift in the Fermi level will affect the equilibrium concentrations of vacancies available. Additionally, coupling between dopant atoms and Si or Ge atoms may significantly affect the interdiffusion behavior of Si and Ge in the structure.

Appendix A

FLOOPS-ISE PROGRAMS USED

A.1 Extraction of Experimental Ge Interdiffusion Profiles

```
# This program is for extracting experimental profiles using effective diffusivity values.
# written by Mohammad Hasanuzzaman under supervision of Dr. Yaser M. Haddara.

# This file contains the coding used to compare extracted experimental Ge interdiffusion profile using
# reported effective diffusivity with the corresponding experimental profile reported by Griglione [47] at
# 1000°C for 43 min anneal in inert ambient.
# When only extraction of Ge interdiffusion profiles are done, only diffusion using the previously reported
# effective diffusivity is performed.

#-------------------------------------------------------------------------#
#---Defining the diffusion model and the effective diffusivity---#
#-------------------------------------------------------------------------#
pdbSetSwitch     Silicon  Dopant  DiffModel      Fermi
pdbSetDoubleArray        Silicon  Germanium      Int      D {0     {0}      1        {0}}
pdbSetDoubleArray        Silicon  Germanium      Vac      D {0     {3e-16}  1        {0}}


#---------------------------------------#
#------ Initializing the structure------#
#---------------------------------------#
line x loc=0.0 tag=surf spac=0.003
line x loc=0.05 tag=cap spac=0.003
line x loc=0.10 tag=sige spac=0.005
line x loc=0.20 tag=buffer spac=0.003
line x loc=0.25 tag=back spac=1

region Silicon xlo=surf xhi=back
init
```

```
#----------------------------------#
#------Initializing profiles------#
#----------------------------------#
#Reading the as-grown SIMS profile of Ge from file and plotting the as-grown profile
profile name=Germanium infile=/home/mhzaman/DBtest/simulation/asgrownSIMS.txt
sel     z=log10(Germanium)
plot.1d  label=Initial_Germanium  !cle     color=blue


# Reading the annealed experimental Ge profile and plotting it to compare with the simulated extracted Ge
# profile
profile name=annealed    infile=/home/mhzaman/DBtest/simulation/annealed.txt
sel     z=log10(annealed)
plot.1d  label=Annealed_experimental      !cle     color=green


#-------------------------------------------------------------------#
#------------------- Performing diffusion--------------------#
#-------------------------------------------------------------------#
diffuse  time=43<min>   temp=1000<C>


#-------------------------------------------------------------------#
#-- Plotting simulated diffused Ge interdiffusion profile --#
#-------------------------------------------------------------------#
sel     z=log10(Germanium)
plot.1d label=Simulated_profile     !cle     color=black symb=v color=red


#-----------------------------------------------------------------------------#
#-- Printing simulated diffused Ge interdiffusion profile to a file--#
#-----------------------------------------------------------------------------#
print.data name=Germanium        outfile=/home/mhzaman/floops/profile/fermiprofilefit.txt
```

A.2 Sample Coding for Applying Vacancy Exchange Mechanism

```
# This program is for simulating Vacancy Exchange Mechanism for samples annealed in inert ambient
# at 1000°C for 125 min.
# written by Mohammad Hasanuzzaman under supervision of Dr. Yaser M. Haddara.


#-----------------------------------------#
#-----Defining boundary conditions----#
#-----------------------------------------#
pdbSetSwitch    Silicon  Dopant  DiffModel       Pair
pdbSetSwitch    Gas_Silicon      Vac     BoundaryCondition       Natural
pdbSetSwitch    Gas_Silicon      Int     BoundaryCondition       Natural
pdbSet  Silicon  Int      Kbulk   1e-10
pdbSet  Gas_Silicon      Vac     Ksurf   1e2
pdbSet  Gas_Silicon      Int     Ksurf   1e2
```

```
#----------------------------------------#
#------ Initializing the structure------#
#----------------------------------------#
line x loc=0.0 tag=surf spac=0.003
line x loc=0.05 tag=cap spac=0.003
line x loc=0.10 tag=sige spac=0.005
line x loc=0.20 tag=buffer spac=0.003
line x loc=100 tag=back   spac=1

region Silicon xlo=surf xhi=back
init

#----------------------------------------------------------------#
#---Adding self defined solution names to solution list---#
#----------------------------------------------------------------#
# concsi and concge respectively refers to the concentrations of substitutional Si and substitutional Ge
solution name=concsi     !negative          !damp   solve    add
solution name=concge     !negative          !damp   solve    add

#----------------------------------------#
#------Defining model equations------#
#----------------------------------------#
# Defining equation of substitutional Si
pdbSetString     Silicon  concsi   Equation          "$c-concge-Vac-concsi"

# Defining equation of substitutional Ge
pdbSetString     Silicon  concge   Equation          "ddt(concge)+((0.4e-13 * concge * (1/c1) * concge *\
(1/c1)+0.005e-13 * concge * (1/c1)+0.003e-13)* ((concge * grad(Vac/Cv))-((Vac/Cv) * grad(concge))))"

# Replacing the default model of vacancy in FLOOPS-ISE with the model equation
pdbSetString     Silicon  Vac      EquationProc     MyDefectBulk
proc     MyDefectBulk     {mat     sol}     {
         set      pdbMat   [pdbName         $mat]
         pdbSetString     $pdbMat          $sol      Equation "ddt(Vac)-(((0.5e-16 * concge *\
(1/c1)+0.3e-16) * (concsi * grad(Vac/Cv)-(Vac/Cv) * grad(concsi)))+((0.4e-13 * concge * (1/$c) * concge\
* (1/c1)+0.005e-13 * concge * (1/c1)+0.003e-13) * ((concge * grad(Vac/Cv))-((Vac/Cv) *\
grad(concge)))))  +1e-10 * (Vac * Int-Cv * EqInt)"
}


#----------------------------------#
#------Initializing profiles------#
#----------------------------------#
# annealed represents the extracted experimental Ge interdiffusion profile and plotting the profile
profile name=annealed     inf=/home/mhzaman/floops/profile/inertdata1000_125.txt
sel      z=log10(annealed)
plot.1d  label=Extracted_experimental      !cle      color=green

# Initializing concge with as-grown Ge profile and plotting the profile
profile name=concge       inf=/home/mhzaman/floops/asgrownSIMS.txt
sel      z=log10(concge)
plot.1d  label=As-grown_Ge       !cle      color=brown

# Cv represents the intrinsic equilibrium vacancy concentration
profile name=Cv  inf=/home/mhzaman/floops/vacdata_1000.txt
```

```
# Vac represents vacancy. Initializing with the equilibrium values
profile name=Vac inf=/home/mhzaman/floops/vacdata_1000.txt

#c1 represents the total number of lattice sites
profile name=c1 inf=/home/mhzaman/floops/c.txt

#-------------------------------------------------------------#
#------------------ Performing diffusion--------------------#
#-------------------------------------------------------------#
diffuse   time=125<min>  temp=1000<C>

#-------------------------------------------------------------#
#-- Plotting simulated diffused Ge interdiffusion profile --#
#-------------------------------------------------------------#
sel       z=log10(concge)
plot.1d  label=Simulated_profile   !cle      color=blue        symb=#

#-------------------------------------------------------------#
#-- Printing simulated diffused Ge interdiffusion profile to a file--#
#-------------------------------------------------------------#
print.data name=concge    outfile=/home/mhzaman/final/output/inertge1000_125.txt
```

A.3 Sample Coding for Mathematical Model Considering the Effects of Interstitials and Vacancies Together

a) Oxidizing Ambient

```
# This program is for simulating mathematical model considering the effects of interstitials along with
# vacancies. Samples are annealed in oxidizing ambient at 1100°C for 4 min.
# written by Mohammad Hasanuzzaman under supervision of Dr. Yaser M. Haddara.

#-----------------------------------------#
#-----Defining boundary conditions----#
#-----------------------------------------#
pdbSetSwitch     Silicon  Dopant  DiffModel        Pair
pdbSetSwitch     Oxide_Silicon    Vac     BoundaryCondition        Natural
pdbSetSwitch     Oxide_Silicon    Int     BoundaryCondition        Natural
pdbSet   Oxide_Silicon    Vac     Ksurf   1e2
pdbSet   Oxide_Silicon    Int     Ksurf   1e2

#-----------------------------------------#
#------ Initializing the structure------#
#-----------------------------------------#
line x loc=0.0 tag=surf spac=0.003
line x loc=0.05 tag=cap spac=0.003
line x loc=0.10 tag=sige spac=0.005
line x loc=0.20 tag=buffer spac=0.003
line x loc=100 tag=back   spac=1

region Silicon xlo=surf xhi=back
init
```

```
#-----------------------------------------------#
#------Initializing model parameters------#
#-----------------------------------------------#
# rKO and rIV respectively represents capture radius of kick-out and recombination mechanism
        set     rKO     0.5e-7
        set     rIV     0.5e-7

# Dgei and Dsii respectively represents diffusivity of interstitial Ge and interstitial Si
        set     Dgei    1.31957e-6
        set     Dsii    1.31957e-6

# Kr_KO and Kf_KO respectively are reverse and forward reaction rates of kick-out mechanism
        set     Kr_KO   "4*3.143*$rKO*$Dgei"
        set     Kf_KO   "4*3.143*$rKO*$Dsii"

# Kf_FT_Si and Kf_FT_Ge respectively are forward reaction rates of recombination mechanism of Si and
# Ge
        set     Kf_FT_Si        "4*3.143*$rIV*($Dsii+5.075e-5)"
        set     Kf_FT_Ge        "4*3.143*$rIV*($Dgei+5.075e-5)"


#-----------------------------------------------------------------#
#---Adding self defined solution names to solution list---#
#-----------------------------------------------------------------#
# concsi and concge respectively refers to the concentrations of substitutional Si and substitutional Ge
# cgei is concentration of interstitial Ge
# eqint and eqcgei respective are equilibrium values of Si interstitial and Ge interstitial
solution name=concsi    !negative       !damp   solve   add
solution name=concge    !negative       !damp   solve   add
solution name=cgei      !negative       !damp   solve   add
solution name=eqint     !negative       !damp   solve   add
solution name=eqcgei    !negative       !damp   solve   add

#-----------------------------------------#
#------Defining model equations------#
#-----------------------------------------#
# Defining equation of substituitional Ge
pdbSetString    Silicon concge  Equation        "-ddt(concge)+((0.1825e-12 * (concge/c1) *\
(concge/c1)+0.02139e-12 * (concge/c1)+0.003e-12) * ((Vac/Cv) * grad(concge)-concge * grad(Vac/Cv)))\
-$Kf_KO * concge * Int+$Kr_KO * concsi * cgei+$Kf_FT_Ge * (cgei * Vac-eqcgei * Cv)"

# Defining equation of substituitional Si
pdbSetString    Silicon concsi  Equation        "$c-concge-Vac-concsi"

# Defining equation of interstitial Ge
pdbSetString    Silicon cgei    Equation        "-ddt(cgei)+($Dgei*eqcgei * grad(cgei/eqcgei))\
+$Kf_KO * concge * Int-$Kr_KO * concsi * cgei-$Kf_FT_Ge * (Vac * cgei-Cv * eqcgei)"

# Replacing the default model of interstitial Si in FLOOPS ISE with the model equation
pdbSetString    Silicon Int     EquationProc    MyDefectBulk1
proc    MyDefectBulk1   {mat    sol}    {
        set     pdbMat  [pdbName        $mat]
        set     rKO     0.5e-7
        set     rIV     0.5e-7
        set     Dgei    1.31957e-6
        set     Dsii    1.31957e-6
```

```
        set     Kr_KO  "4*3.143*$rKO*$Dgei"
        set     Kf_KO  "4*3.143*$rKO*$Dsii"
        set     Kf_FT_Si        "4*3.143*$rIV*($Dsii+5.075e-5)"
        set     Kf_FT_Ge        "4*3.143*$rIV*($Dgei+5.075e-5)"

        pdbSetString    $pdbMat         $sol    Equation "-ddt(Int)+$Dsii*eqint*grad(Int/eqint)\
-$Kf_KO * concge * Int+$Kr_KO * concsi * cgei-$Kf_FT_Si * (Vac * Int-Cv * eqint)"
}


# Replacing the default model of vacancy in FLOOPS-ISE with the model equation
pdbSetString    Silicon Vac     EquationProc    MyDefectBulk
proc    MyDefectBulk    {mat    sol}    {
        set     pdbMat  [pdbName        $mat]
        set     rKO     0.5e-7
        set     rIV     0.5e-7
        set     Dgei    1.31957e-6
        set     Dsii    1.31957e-6
        set     Kr_KO  "4*3.143*$rKO*$Dgei"
        set     Kf_KO  "4*3.143*$rKO*$Dsii"
        set     Kf_FT_Si        "4*3.143*$rIV*($Dsii+5.075e-5)"
        set     Kf_FT_Ge        "4*3.143*$rIV*($Dgei+5.075e-5)"


        pdbSetString    $pdbMat         $sol    Equation "-ddt(Vac)+((0.1825e-12 * (concge/c1) *\
(concge/c1)+0.02139e-12 * (concge/c1)+0.003e-12) * (concge * grad(Vac/Cv)-(Vac/Cv) *\
grad(concge))+(0.375e-15 * (concge/c1)+0.5e-15) * (concsi * grad(Vac/Cv)-(Vac/Cv) * grad(concsi)))\
-$Kf_FT_Ge * (Vac * cgei-Cv * eqcgei)-$Kf_FT_Si * (Vac * Int-Cv * eqint)"
}

# Defining values for equilibrium interstitial Ge
pdbSetString    Silicon eqcgei  Equation        "eqcgei-1e-2 *eqint"

# Defining values for equilibrium interstitial Si
pdbSetString    Silicon eqint   Equation        "eqint-9.62e13  *  exp(-99.54  *  (concge/c1)  *\
(((((concge/c1) * 5.66+(1-(concge/c1)) * 5.43)-5.43)/5.43)))"


#-----------------------------------#
#------Initializing profiles------#
#-----------------------------------#
# annealed represents the extracted experimental Ge interdiffusion profile and plotting the profile
profile name=annealed   inf=/home/mhzaman/floops/profile/oxdata1100_4.txt
sel     z=log10(annealed)
plot.1d  label=Extracted_experimental    !cle    color=pink      max=0.25

# Initializing concge with as-grown Ge profile and plotting the profile
profile name=concge     inf=/home/mhzaman/floops/asgrownSIMS.txt
sel     z=log10(concge)
plot.1d  label=As-grown_Ge      !cle    color=red       max=0.25

# Cv represents the inert equilibrium vacancy concentration
profile name=Cv inf=/home/mhzaman/floops/vacdata_1100.txt

# Vac represents vacancy. Initializing with the equilibrium values
profile name=Vac inf=/home/mhzaman/floops/vacdata_1100.txt
```

```
#c1 represents the total number of lattice sites
profile name=c1 inf=/home/mhzaman/floops/c.txt

#-------------------------------------------------------------#
#------------------ Performing diffusion--------------------#
#-------------------------------------------------------------#
diffuse   time=4<min>     temp=1100<C>   O2


#-------------------------------------------------------------#
#-- Plotting simulated diffused Ge interdiffusion profile --#
#-------------------------------------------------------------#
sel       z=log10(concge)
plot.1d   label=Simulated_profile   !cle      color=blue        symb=# max=0.25


#-----------------------------------------------------------------------#
#-- Printing simulated diffused Ge interdiffusion profile to a file--#
#-----------------------------------------------------------------------#
print.data name=concge    outfile=/home/mhzaman/new/output/oxout1100_4.txt
```

b) Nitriding Ambient

```
# This program is for simulating mathematical model considering the effects of interstitials along with
# vacancies. Samples are annealed in nitriding ambient at 1100°C for 4 min.
# written by Mohammad Hasanuzzaman under supervision of Dr. Yaser M. Haddara.

#-----------------------------------------#
#-----Defining boundary conditions----#
#-----------------------------------------#
pdbSetSwitch     Silicon  Dopant  DiffModel        Pair
pdbSetSwitch     Nitride_Silicon  Vac     BoundaryCondition        Natural
pdbSetSwitch     Nitride_Silicon  Int     BoundaryCondition        Natural
pdbSet   Nitride_Silicon  Vac     Ksurf   1e2
pdbSet   Nitride_Silicon  Int     Ksurf   1e2


#-----------------------------------------------------#
#----------Vacancy Injection Equations---------#
#-----------------------------------------------------#
pdbSetString Nitride_Silicon Vac EquationProc MySurfEquation
proc     MySurfEquation  {mat     sol} {
         set pdbMat      [pdbName        $mat]
         pdbSetString    $pdbMat         $sol     Equation_Silicon "6e9-1.5e-3*(Vac_Silicon\
-EqVac_Silicon)"
}
```

```
#-----------------------------------------#
#------ Initializing the structure------#
#-----------------------------------------#
line x loc=-0.01 tag=nit spac=0.003
line x loc=0.0 tag=surf spac=0.003
line x loc=0.05 tag=cap spac=0.003
line x loc=0.10 tag=sige spac=0.005
line x loc=0.20 tag=buffer spac=0.003
line x loc=100 tag=back    spac=1

region Nitride xlo=nit xhi=surf
region Silicon xlo=surf xhi=back
init

#-------------------------------------------------#
#------Initializing model parameters------#
#-------------------------------------------------#
# rKO and rIV respectively represents capture radius of kick-out and recombination mechanism
        set     rKO     0.5e-7
        set     rIV     0.5e-7

# Dgei and Dsii respectively represents diffusivity of interstitial Ge and interstitial Si
        set     Dgei    1.91957e-6
        set     Dsii    1.91957e-6

# Kr_KO and Kf_KO respectively are reverse and forward reaction rates of kick-out mechanism
        set     Kr_KO   "4*3.143*$rKO*$Dgei"
        set     Kf_KO   "4*3.143*$rKO*$Dsii"

# Kf_FT_Si and Kf_FT_Ge respectively are forward reaction rates of recombination mechanism of Si and
# Ge
        set     Kf_FT_Si        "4*3.143*$rIV*($Dsii+5.075e-5)"
        set     Kf_FT_Ge        "4*3.143*$rIV*($Dgei+5.075e-5)"


#-----------------------------------------------------------------#
#---Adding self defined solution names to solution list---#
#-----------------------------------------------------------------#
# concsi and concge respectively refers to the concentrations of substitutional Si and substitutional Ge
# cgei is concentration of interstitial Ge
# eqint and eqcgei respective are equilibrium values of Si interstitial and Ge interstitial
solution name=eqcgei    !negative       !damp   solve   add
solution name=concsi    !negative       !damp   solve   add
solution name=concge    !negative       !damp   solve   add
solution name=cgei      !negative       !damp   solve   add
solution name=eqint     !negative       !damp   solve   add


#-----------------------------------------#
#------Defining model equations------#
#-----------------------------------------#
# Defining equation of substituitional Ge
pdbSetString    Silicon  concge  Equation        "-ddt(concge)+((0.1825e-12 * (concge/c1) *\
(concge/c1)+0.02139e-12 * (concge/c1)+0.003e-12) * ((Vac/Cv) * grad(concge)-concge * grad(Vac/Cv)))\
-$Kf_KO * concge * Int+$Kr_KO * concsi * cgei+$Kf_FT_Ge * (cgei * Vac-eqcgei * Cv)"
```

```
# Defining equation of substituitional Si
pdbSetString    Silicon  concsi   Equation        "$c-concge-Vac-concsi"

# Replacing the default model of interstitial Si in FLOOPS ISE with the model equation
pdbSetString    Silicon  Int      EquationProc    MyDefectBulk1
proc    MyDefectBulk1  {mat    sol}    {
        set     pdbMat  [pdbName       $mat]
        set     rKO     0.5e-7
        set     rIV     0.5e-7
        set     Dgei    1.31957e-6
        set     Dsii    1.91957e-6
        set     Kr_KO   "4*3.143*$rKO*$Dgei"
        set     Kf_KO   "4*3.143*$rKO*$Dsii"
        set     Kf_FT_Si        "4*3.143*$rIV*($Dsii+5.075e-5)"
        set     Kf_FT_Ge        "4*3.143*$rIV*($Dgei+5.075e-5)"

        pdbSetString    $pdbMat         $sol    Equation        "-ddt(Int)+$Dsii*eqint*grad(Int/eqint)\
-$Kf_KO*concge*Int+$Kr_KO*concsi*cgei-$Kf_FT_Si*(Vac*Int-Cv*eqint)"
}

# Replacing the default model of vacancy in FLOOPS-ISE with the model equation
pdbSetString    Silicon  Vac      EquationProc    MyDefectBulk
proc    MyDefectBulk   {mat    sol}    {
        set     pdbMat  [pdbName       $mat]
        set     rKO     0.5e-7
        set     rIV     0.5e-7
        set     Dgei    1.31957e-6
        set     Dsii    1.91957e-6
        set     Kr_KO   "4*3.143*$rKO*$Dgei"
        set     Kf_KO   "4*3.143*$rKO*$Dsii"
        set     Kf_FT_Si        "4*3.143*$rIV*($Dsii+5.075e-5)"
        set     Kf_FT_Ge        "4*3.143*$rIV*($Dgei+5.075e-5)"

        pdbSetString    $pdbMat         $sol    Equation "-ddt(Vac)+((0.1825e-12 * (concge/c1) *\
(concge/c1)+0.0213e-12 * (concge/c1)+0.003e-12) * (concge * grad(Vac/Cv)-(Vac/Cv) *\
grad(concge))+(0.375e-15 * (concge/c1)+0.5e-15) * (concsi * grad(Vac/Cv)-(Vac/Cv) * grad(concsi)))\
-$Kf_FT_Ge * (Vac * cgei-Cv * eqcgei)-$Kf_FT_Si * (Vac * Int-Cv * eqint)"
}

# Defining equation of interstitial Ge
pdbSetString    Silicon  cgei     Equation        "-ddt(cgei)+($Dgei * eqcgei *\
grad(cgei/eqcgei))+$Kf_KO * concge * Int-$Kr_KO * concsi * cgei-$Kf_FT_Ge * (Vac * cgei-Cv *\
eqcgei)"

# Defining values for equilibrium interstitial Ge
pdbSetString    Silicon  eqcgei   Equation        "eqcgei-1e-2*eqint"

# Defining values for equilibrium interstitial Si
pdbSetString    Silicon  eqint    Equation        "eqint-9.62e13  *  exp(-99.54  *  (concge/c1)  *\
(((((concge/c1) * 5.66+(1-(concge/c1)) * 5.43)-5.43)/5.43)))"
```

```
#----------------------------------#
#------Initializing profiles------#
#----------------------------------#
# annealed represents the extracted experimental Ge interdiffusion profile and plotting the profile
profile name=annealed     inf=/home/mhzaman/floops/profile/nitdata1100_4.txt
sel       z=log10(annealed)
plot.1d   label=Annealed_data_from_Fermi  !cle       color=pink        max=0.25

# Initializing concge with as-grown Ge profile and plotting the profile
profile name=concge       inf=/home/mhzaman/floops/asgrownSIMS.txt
sel       z=log10(concge)
plot.1d   label=Initial_concge        !cle       color=red         max=0.25

# Cv represents the inert equilibrium vacancy concentration
profile name=Cv  inf=/home/mhzaman/floops/vacdata_1100.txt

# Vac represents vacancy. Initializing with the equilibrium values
profile name=Vac inf=/home/mhzaman/floops/vacdata_1100.txt

#c1 represents the total number of lattice sites
profile name=c1 inf=/home/mhzaman/floops/c.txt

#-------------------------------------------------------------#
#------------------ Performing diffusion--------------------#
#-------------------------------------------------------------#
diffuse   time=4<min>     temp=1100<C>


#-------------------------------------------------------------#
#-- Plotting simulated diffused Ge interdiffusion profile --#
#-------------------------------------------------------------#
sel       z=log10(concge)
plot.1d   label=Final_concge        !cle       color=blue        symb=# max=0.25

#-------------------------------------------------------------------------#
#-- Printing simulated diffused Ge interdiffusion profile to a file--#
#-------------------------------------------------------------------------#
print.data name=concge    outfile=/home/mhzaman/new/output/nitout1100_4.txt
```

A.4 Sample Coding for Mathematical Model of Vacancy Injection

```
# This program is for setting vacancy injection parameters for the model proposed for vacancy injection
# at nitriding ambient.
# written by Mohammad Hasanuzzaman under supervision of Dr. Yaser M. Haddara.

pdbSetSwitch Silicon Dopant DiffModel Pair
```

```
#-----------------------------------------#
#------Setting vacancy diffusivity------#
#-----------------------------------------#
pdbSet   Silicon   VacancyD        {0        {8e-12}}

#-------------------------------------------------#
#------Setting vacancy injection equation------#
#-------------------------------------------------#
pdbSet Nitride_Silicon Vac EquationProc    MySurfEquation

proc     MySurfEquation  {mat     sol} {
         set pdbMat        [pdbName        $mat]
         pdbSetString      $pdbMat         $sol      Equation_Silicon "1.2e1-5e-10*(Vac_Silicon-\
EqVac_Silicon)"
}

#---------------------------------------#
#------ Initializing the structure------#
#---------------------------------------#
line x loc=-0.1 tag=nit
line x loc=0.0 tag=surf spac=0.003
line x loc=1500.0 tag=back

region Nitride xlo=nit xhi=surf
region Silicon xlo=surf xhi=back
init


#-------------------------------------#
#------Performing diffusion------#
#-------------------------------------#
set tsum 0
set sum 0
set i 0
set a 0
set timeprev(0) 0
set cv(0) 1.367271e8
set cveq 1.367271e8

set k 1
set l 0


diffuse   time=60.0<min>  temp=810<C>     movie = {
select    z=Vac

# Measuring values at the depth of 0.15 microns
set aslist [lindex [slice x=0] 0]
while {$i>=0} {

         set c [lindex $aslist $i]
         incr i 2
         set d [lindex $aslist $i]

         if {($c <= 0.15) && ($d >=0.15)} {
         incr i
```

```
        set e [lindex $aslist $i]
        puts $e
        break
        }
}

set sumstage [expr $sum+(($e+$cv($l)/2.0))*($time-$timeprev($l))]
set sum $sumstage

set tstep [expr $time-$timeprev($l)]
set tsumstep [expr $time-$timeprev($l)+$tsum]
set tsum $tsumstep

incr l
set timeprev($l) $time
set cv($l) $e

set i 0
}

set sumfinal [expr $sum/$tsum]
set enhance [expr $sumfinal/$cveq]

#-------------------------------------------------------#
#------Printing the values of <Cv>/Cv*--------#
#-------------------------------------------------------#
puts $enhance
```

REFERENCES

[1] G. E. Moore, Electronic **38**, (1965).

[2] T. Skotnicki, J. A. Hutchby, T. -J. King, H. -S. P. Wong, and F. Boeuf, IEEE Cir. & Dev. Mag. **21**, 16 (2005).

[3] S. C. Jain, A. H. Harker, and R. A. Cowley, Philos. Mag. A **75**, 1461 (1997).

[4] V. T. Bublik, S. S. Gorelik, A. A. Zaitsev, and A. Y. Polakov, Phys. Stat. Sol B **65**, K79 (1974).

[5] D. J. Paul, Semicon. Sci. Technol. **19**, R75 (2004).

[6] U. König, and A. Gruhle, Proc. IEEE/Cornell Conf. on Advanced Concepts in High Speed Semiconductor Devices and Circuits 1997, p. 14.

[7] J. Wan, Y. H. Luo, Z. M. Jilang, G. Jin, J. L. Liu, and Kang L. Wang, J. Appl. Phys. **90**, 4290 (2001).

[8] FLOOPS-ISE manual, Integrated System Engineering, Release 9.5.

[9] M. Lannoo, and J. Bourgoin, *Point Defects in Semiconductors I* (Springer-Verlag, New York, 1981).

[10] S. Wolf, and R. N. Tauber, *Silicon Processing for the VLSI Era Volume 1- Process Technology* (Lattice Press, Sunset Beach, 1986).

[11] K. H. Nicholas, Solid-State Electron. **9**, 35 (1966).

[12] G. Masetti, S. Solmi, and G. Soncini, Solid-State Electron. **16**, 1419 (1973).

[13] C. Hill, Semiconductor Silicon, 1981, edited by H. R. Huff and R. J. Jriegler, p.500.

[14] R. Francis, and P. S. Dobson, J. Appl. Phy. **50**, 280 (1979).

[15] S. M. Hu, J. Appl. Phys. **45**, 1567 (1974).

[16] S. T. Dunham, and J. D. Plummer, J. Appl. Phys. **59**, 2551 (1986).

[17] S. Mizuo, and H. Higuchi, J. Electrochem. Soc. **130**, 1942 (1983).

[18] M. M. Moslehi, and K. C. Sarawat, IEEE Trans. Elec. Dev. **32**, 106 (1985).

[19] S. T. Ahn, H. W. Kennel, J. D. Plummer, and W. A. Tiller, Appl. Phys. Lett. **53**, 1593 (1988).

[20] S. T. Ahn, H. W. Kennel, J. D. Plummer, and W. A. Tiller, J. Appl. Phys. **64**, 4914 (1988).

[21] R. N. Ghoshtagore, Phys. Rev. Lett. **16**, 890 (1966).

[22] L. Kalinowski and R. Seguin, Appl. Phys. Lett. **35**, 211 (1979).

[23] G. Vogel, G. Hettich, and H. Mehrer, J. Phys. C: Solid State Phys. **16**, 6197 (1983).

[24] M. Werner, H. Mehrer, and H. D. Hochheimer, Phys. Rev. B **32**, 3930 (1985).

[25] D. R. Campbell, Phys. Rev. B **12**, 2318 (1975).

[26] A. Seeger, and K. P Chik, Phys. Stat. Sol. **29**, 455 (1968).

[27] G. Hettich, H. Mehrer, and K. Maier, *Defects and Radiation Effects in Semiconductors 1978*, edited by J. H. Albany, Inst. Phys. Conf. Ser. 46 (Institute of Physics, London, 1979), p. 500.

[28] M. Ogino, Y. Oana, and M. Watanable, Phys. Stat. Sol. A **72**, 535 (1982).

[29] H. Siethoff, and W. Schroeter, Phil. Mag. A **37**, 711 (1978).

[30] P. Dorner, W. Gust, B. Predel, U. Roll, A. Lodding, and H. Odelius, Phil. Mag. A **49**, 557 (1984).

[31] G. L. McVay and A. R. DuCharme, Phys. Rev. B **9**, 627 (1974).

[32] A. Strohm, T. Voss, W. Frank, J. Räisänen, M. Dietrich, Physica B **308-310**, 542 (2001).

[33] P. Laitinen, A. Strohm, J. Huikari, A. Nieminen, T. Voss, C. Grodon, I. Riihimäki, M. Kummer, J. Äystö, P. Dendooven, J. Räisänen, W. Frank, and the ISOLDE Collaboration, Phys. Rev. Lett. **89**, 085903 (2002).

[34] N. R. Zangenberg, J. L. Hanses, J. F-Pedersen, and A. N. Larsen, Phys. Rev. Letts. **87**, 12501 (2001).

[35] H. Sunamura, S. Fukatsu, N. Usami, and Y. Shiraki, Jpn. J. Appl. Phys. **33**, 2344 (1994).

[36] H. Sunamura, S. Fuktsu, N. Usami, and Y. Shiraki, Appl. Phys. Lett. **63**, 1651 (1993).

[37] L. J. van Ijzendoorn, G. F. A. van de Walle, A. A. van Gorkum, A. M. I. Theunissen, R. A. van den Heuvel, and J. H. Barrett, Nuc. Inst. Met. Phys. Res. B **50**, 127 (1990).

[38] G. L. McVay and A. R. DuCharne, J. Appl. Phys. **44**, 1409 (1973).

[39] B. Holländer, R. Butz, and S. Mantl, Phys. Rev. B **46**, 6975 (1992).

[40] J. -M. Baribeau, R. Pascual, and S. Saimoto, Appl. Phys. Lett. **57**, 1502 (1990).

[41] S. J. Chang, K. L. Wang, R. C. Bowman, and P. M. Adams, Appl. Phys. Lett. **54**, 1253 (1989).

[42] S. M. Prokes, O. J. Glembocki, and D. J. Godbey, Appl. Phys. Lett. **60**, 1087 (1992).

[43] M. Griglione, T. J. Anderson, Y. M. Haddara, M. E. Law, K. S. Jones, and A. vanden Bogaard, J. Appl. Phys. **88**, 1366 (2000).

[44] M. Griglione, T. J. Anderson, M. E. Law, K. S. Jones, A. van den Boggard, M. P-Lambers, J. Appl. Phys. **89**, 2904 (2001).

[45] S. S. Iyer, and F. K. LeGoues, J. Appl. Phys. **65**, 4693 (1989).

[46] M. A. Herman, and H. Sitter, *Molecular Beam Epitaxy: Fundamentals and Current Status* (Springer, New York, 1996).

[47] M. D. Griglione, PhD thesis, University of Florida (1999).

[48] A. Benninghoven, F. G. Rudenauer, and H. W. Werner, *Secondary Ion Mass Spectrometry: Basic Concepts, Instrumental Aspects, Applications and Trends* (J. Wiley, New York, 1987).

[49] M. Ohring, *Materials Science of Thin Films: Deposition and Structure* (Academic Press, San Diego, 2002).

[50] E. Kirkendall, L. Thomassen, and C. Upthegrove, Trans. AIME **133**, 186 (1939).

[51] A. D. Smigelskas and E. O. Kirkendall, Trans. AIME **171**, 130 (1947).

[52] L. S. Darken, Trans. AIME **175**, 184 (1984).

[53] C. -Y. Tai, PhD Thesis, Stanford University (1997).

[54] M. P. Chase, C. -Y. Tai, M. D. Deal, and Y. M. Haddara, *Private Communication of the Interdiffusion Mechanisms* (Stanford University, 1996-1997).

[55] J. L. Ngau, P. B. Griffin, and J. D. Plummer, J. Appl. Phys. **90**, 1768 (2001).

[56] A. Pakfar, Materials Science and Engineering B **89**, 225 (2002).

[57] M. J. Aziz, Appl. Phys. Lett. **70**, 2810 (1997).

[58] Richard J. Borg, and G. J. Dienes, *An Introduction to Solid State Diffusion* (Academic Press Inc., Boston, 1998).

[59] B. L. Sharma, Defect and Diffusion Forum **70-71**, 1 (1990).

[60] T. K. Mogi, M. O. Thompson, H. -J. Gossmann, J. M. Poate, and H. S. Luftman, Appl. Phys. Lett. **69**, 1273 (1996).

[61] P. Fahey, G. Barbuscia, M. Moslehi, and R. W. Dutton, Appl. Phys. Lett. **46**, 784 (1985).